Shear Strength Model for FRP-Strengthened RC Beams with Adverse FRP-Steel Interaction

G. M. Chen [1]; J. G. Teng [2] ; and J. F. Chen [3]

Abstract: RC beams shear-strengthened with externally-bonded FRP U-strips or side strips usually fail due to debonding of the bonded FRP shear reinforcement. Because such debonding usually occurs in a brittle manner at relatively small shear crack widths, some of the internal steel stirrups intersected by the critical shear crack may not have reached yielding at beam shear failure. Consequently, the yield strength of internal steel stirrups in such a strengthened RC beam cannot be fully utilized. This adverse shear interaction between the internal steel shear reinforcement and the external FRP shear reinforcement may significantly reduce the benefit of the shear-strengthening FRP but has not been considered explicitly by any of the shear strength models in the existing design guidelines. This paper presents a new shear strength model considering this adverse shear interaction through the introduction of a shear interaction factor. A comprehensive evaluation of the proposed model, as well as three other shear strength models, is conducted using a large test database. It is shown that the proposed shear strength model performs the best among the models compared, and the performance of the other shear strength models can be significantly improved by including the proposed shear interaction factor. Finally, a design recommendation is presented.

CE Database subject headings: Fiber reinforced polymer; Reinforced Concrete; Concrete beams; Bonding; Shear failures; Shear resistance; Shear strength.

[1] Postdoctoral Fellow, Department of Civil and Structural Engineering, The Hong Kong Polytechnic University, Hong Kong, China
[2] Chair Professor of Structural Engineering, Department of Civil and Structural Engineering, The Hong Kong Polytechnic University, Hong Kong, China (Corresponding author); Email: cejgteng@polyu.edu.hk
[3] Reader, Institute for Infrastructure and Environment, School of Engineering, The University of Edinburgh, Edinburgh, U.K.

INTRODUCTION

The external bonding of fiber-reinforced polymer (FRP) to reinforced concrete (RC) structures has become a popular strengthening technique in the past decade; the technique has also received much research attention (Bank 2006; Hollaway and Teng 2008; Oehlers and Seracino 2004; Teng et al. 2002). In particular, the shear resistance of RC beams can be enhanced by bonding FRP shear reinforcement in the forms of complete wraps, U-jackets and side strips (Chen and Teng 2003a, b; Teng et al. 2002). Without loss of generality, the FRP shear reinforcement is assumed herein to be in the form of discrete strips for ease of discussion; a continuous sheet with fibres oriented in a single direction can be treated as discrete strips in the fibre direction with a zero net gap between strips.

Existing research has established a general picture of the structural behaviour of RC beams shear-strengthened with FRP and led to a number of shear strength models for them (Chen and Teng 2003a, b; Khalifa et al. 1998; Monti and Liotta 2007; Triantafillou 1998; Triantafillou and Antonopoulos 2000); the more reliable of these shear strength models have been adopted by design guidelines (ACI-440.2R 2008; CNR-DT200 2004; fib 2001; HB305 2008). A comprehensive review of existing work (Chen 2010), however, reveals that several aspects of the behaviour of such strengthened beams are still not well understood. In particular, the adverse interaction between the different components of shear resistance (Ali et al. 2006; Chen et al. 2010; Pellegrino and Modena 2002, 2006, 2008) has been identified as a major issue that requires further research.

This paper deals with the effect of interaction between the internal steel shear reinforcement (only stirrups are considered to simplify the problem) and the external FRP shear reinforcement in RC beams shear-strengthened with FRP U-strips or side strips. Such strengthened beams commonly fail due to the debonding of FRP strips from the beam sides (Chen and Teng 2003b; Teng and Chen 2009). This failure mode is usually brittle so that the width of the critical shear crack is limited when FRP debonding occurs (Ali et al. 2006; Chen et al. 2010; Pellegrino and Modena 2008). As a result, at the instance of debonding failure, the component of shear resistance from concrete is likely to be well maintained (e.g. Bousselham and Chaallal 2008), but the component of shear resistance from steel may be significantly below what is expected in a conventional RC beam because not all steel stirrups in an FRP-strengthened RC beam intersected by the critical shear crack can reach yielding at the shear failure of the beam (Ali et al. 2006; Chen et al. 2010; Deniaud and Cheng 2001; Li et al. 2002; Monti and Liotta 2007; Pellegrino and Modena 2008; Teng et al. 2002; Teng et al. 2004). It may be noted that this adverse shear interaction effect has not been duly considered in any of the existing design guidelines (Chen 2010).

Shear strength models in existing guidelines are based on the simple additive approach that the shear resistance of a shear-strengthened RC beam can be found from the following equation::

$$V_u = V_c + V_s + V_f \tag{1}$$

where V_c, V_s and V_f are the components contributed by the concrete, the steel shear reinforcement, and the FRP shear reinforcement respectively. The values of V_c and V_s are generally evaluated using provisions in existing design codes for RC structures, while various expressions have been proposed for V_f. Eq. (1) implies that the three shear resistance components reach their ultimate values simultaneously in a real beam, which is over-optimistic and un-conservative.

A number of studies have been conducted to consider the shear interaction issue (e.g. Ali et al. 2006; Li et al. 2001; Pellegrino and Modena 2002, 2006, 2008), leading to several shear strength models that consider the shear interaction effect (Li et al. 2001;

Pellegrino and Modena 2002, 2006, 2008). These models, however, have been developed on the basis of limited experimental results and thus suffer from inevitable limitations. Recently, Modifi and Chaallal (2011) proposed a new shear strength model that accounts for this adverse shear interaction effect by introducing the so-called cracking modification factor (β_c) which is related to the rigidities of both steel shear reinforcement and FRP shear reinforcement; the expression of β_c was determined by curve-fitting of the experimental results for V_f. These authors have shown that the inclusion of β_c can improve the performance of the proposed shear strength model as well as some other shear strength models. Whilst the work represents a valuable step forward in understanding and modeling the FRP-steel interaction effect, their model requires improvement, especially for beams with FRP U-strips where the FRP shear contribution (V_f) is significantly overestimated for a large number of specimens.

To understand the interaction between the three components of shear resistance in Eq. (1), it is necessary to investigate how each of them develops during the loading process. If these components are quantified during the loading process, the shear resistance of the beam can also be quantified throughout the loading process and its ultimate value can be obtained by finding the maximum of the sum of the three components as schematically shown in Fig. 1. The authors have recently employed a theoretical approach to establish the development of shear contributions from the FRP (Chen et al. 2011) and the steel stirrups (Chen et al. 2010) throughout the loading process as characterized by the critical shear crack width. This paper first presents a shear strength model for FRP debonding failure considering the adverse FRP-steel shear interaction developed based on the work presented in Chen et al. (2010; 2011). Its performance is then assessed using a large test database collected from the literature. A simplified design recommendation is finally presented.

SHEAR STRENGTH MODEL ACCOUNTING FOR FRP-STEEL INTERACTION

As with most of the shear strength models in existing guidelines, the proposed shear strength model is based on the assumption that the shear failure of an FRP shear-strengthened RC beam is dominated by a single critical shear crack as schematically shown in Fig. 2, and the shear contributions of both FRP strips and steel stirrups can be evaluated by truss analogy.

As discussed earlier, the contributions from the concrete, internal steel stirrups and external FRP strips develop gradually during the loading process (Fig. 1). For FRP debonding failure, it may be assumed that the contribution of concrete to the shear capacity of the beam (V_c) is the same as that in an un-strengthened RC beam because the width of the critical shear crack is likely to be small when the beam fails due to FRP debonding (Bousselham and Chaallal 2008). Therefore, the shear resistance of the beam can be expressed as [instead of Eq. (1)]:

$$V_u = V_c + K_s V_{s,p} + K_f V_{f,p} \tag{2}$$

where $V_{s,p}$ and $V_{f,p}$ are the maximum shear contributions of steel stirrups and FRP strips respectively, K_s and K_f are mobilization factors for the steel stirrups and FRP strips respectively which have been defined by Chen et al. (2010) as:

$$K_s = \sigma_{s,e} / f_y \tag{3}$$

$$K_f = \sigma_{f,e} / f_{f,e} \tag{4}$$

in which $\sigma_{s,e}$ and $\sigma_{f,e}$ are respectively the average stress in the steel stirrups and FRP strips intersected by the critical shear crack, f_y is the yield strength of the steel stirrups, and $f_{f,e}$ is the effective (average) stress in the FRP intersected by the critical shear crack when V_f peaks (i.e. $V_f = V_{f,p}$, which does not necessarily correspond to the ultimate state of the

beam as shown in Fig. 1).

K_s and K_f are respectively proportional to the average stress in the steel stirrups and that in the FRP strips, which are in turn directly related to the shear crack width w. Clearly, K_s and K_f reflect the degree of mobilization of the steel stirrups and that of the FRP strips respectively in resisting shear at a given load level or a shear crack width and capture the interaction between steel stirrups and FRP strips in resisting shear.

Development of the FRP Contribution K_fV_f with crack width

It shall be noted that in both the numerical study (Chen et al. 2010) and analytical solution (Chen et al. 2011) on which the present study is based, it was assumed that the width of the critical shear crack varies linearly from the crack tip to the crack end; this assumption normally leads to conservative results for both FRP strips and steel stirrups (Chen 2010). With this assumption, the maximum value of the shear crack width is always at the crack end (Fig. 2); this value is referred to as the crack end width and is represented by w_e in this paper. In Chen et al. (2010, 2011), it was also assumed that the upper end (i.e. the crack tip) of the critical shear crack at the ultimate state is located at $0.1d$ from the compression face of the beam (see Fig. 2), with d being the effective depth of the beam.

Based on the above assumptions and the full-range behaviour of FRP-to-concrete bonded joints, Chen et al. (2011) developed closed-formed solutions for the development of the shear contribution of FRP (V_f) with the crack end width (w_e) for both FRP U-strips and side strips. Figure 3 shows example $V_f - w_e$ curves, where the peak loads are denoted by P_u and P_s respectively for FRP U-strips and side strips. From the $V_f - w_e$ curve, the $K_f - w_e$ curve can be easily obtained according to Eq. (3). Figure 4 shows the $K_f - w_e$ curves corresponding to the $V_f - w_e$ curves in Fig. 3. Chen et al. (2011) demonstrated that the $K_f - w_e$ curve depends mainly on the FRP stiffness $E_f t_f$ and the beam height (which can be represented by the effective height of FRP $h_{f,e}$ as shown in Fig. 2).

The maximum FRP contribution $V_{f,p}$ (the peak value on the $V_f - w_e$ curve) can be obtained by setting $\partial V_f / \partial w_e = 0$ based on the $V_f - w_e$ relationship presented in Chen et al. (2011). The general expression for $V_{f,p}$ is given as (Chen et al. 2011):

$$V_{f,p} = 2 f_{f,e} t_f w_f \frac{h_{f,e}\left(\cot\theta + \cot\beta\right)\sin\beta}{s_f} \tag{5}$$

$$f_{f,e} = \sigma_{f,\max}\, D_{frp} \tag{6}$$

$$\sigma_{f,\max} = \min\begin{cases} f_f \\ \sigma_{db,\max} \end{cases} \tag{7a}$$

$$\sigma_{db,\max} = \begin{cases} \sqrt{\dfrac{2E_f G_f}{t_f}} & L_{\max} \geq L_e \\ \sin\left(\dfrac{\pi}{2}\cdot\dfrac{L}{L_e}\right)\sqrt{\dfrac{2E_f G_f}{t_f}} & L_{\max} < L_e \end{cases} \tag{7b}$$

$$L_{\max} = \begin{cases} \dfrac{h_{f,e} + h_t + h_b}{2\sin\beta} & \text{for side strips} \\ \dfrac{h_{f,e} + h_t + h_b}{\sin\beta} & \text{for U - strips} \end{cases} \tag{7c}$$

where $f_{f,e}$ is the effective (average) stress in the FRP intersected by the critical shear crack; w_f is the width of individual FRP strips perpendicular to the fiber direction (all FRP strips are assumed to have the same w_f); s_f is the centre-to-centre spacing of FRP strips measured along the longitudinal axis of the beam (the FRP strips are assumed to be evenly distributed; and thus for an FRP continuous sheet, $s_f = w_f / \sin\beta$.); t_f is the FRP strip thickness; θ is the angle between the critical shear crack and the longitudinal beam axis; β is the angle between the fiber direction and the longitudinal beam axis; $\sigma_{f,\max}$ is the maximum stress in the FRP strips intersected by the critical shear crack; $\sigma_{db,\max}$ is the maximum stress in the FRP strips intersected by the critical shear crack as governed by debonding failure; $L_{\max}$ is the maximum bond length of FRP strips intersected by the critical shear crack; L_e is **t**he effective bond length of FRP strips as defined by Eq. (16); h_b is the thickness of concrete cover (from the beam bottom to the crack end) (see Fig 2); h_t is the vertical distance from the top of FRP strips to the crack tip (see Fig 2); and D_{frp} is the stress/strain distribution factor determined according to Chen et al. (2011) as follows.

For FRP side strips, the expression of D_{frp} is given by

$$D_{frp} = 1 - (1 - \frac{\pi}{4}) \cdot \frac{h_{df}}{h_{f,e}} - \frac{h_{db}}{h_{f,e}} \tag{8}$$

$$h_{df} = \frac{h_{f,e} - h_{db}}{1 + \frac{\pi}{2}(k_h - 1)} \tag{9}$$

$$h_{db} = L_m \sin\beta - h_b \tag{10}$$

$$L_m = k_h \cdot L_e \tag{11}$$

$$k_h = \frac{2}{\pi}\sqrt{\left(1 - \frac{\pi}{4}\right)\left(1 - \frac{\pi}{2}\right) + \frac{\pi}{2}\left(1 - \frac{\pi}{4}\right)\frac{(h_{f,e} + h_b)}{L_e \sin\beta}} + 1 - \frac{2}{\pi} \tag{12}$$

For FRP U-strips, the expression of D_{frp} is given by

$$D_{frp} = 1 - (1 - \frac{\pi}{4}) \cdot \frac{h_{df}}{h_{f,e}} \tag{13}$$

$$h_{df} = 2\delta_f \cdot \frac{h_{f,e}}{w_{e,p}\sin(\theta + \beta)} \tag{14}$$

$$w_{e,p} = \delta_f \cdot \frac{1 + \frac{\pi}{2}\left(\frac{h_{f,e}}{L_e \sin\beta} - 1\right)}{\sin(\theta + \beta)} \tag{15}$$

$$L_e = \sqrt{\frac{\tau_f}{\delta_f E_t t_f}} \tag{16}$$

$$\delta_f = 2G_f / \tau_f \tag{17}$$

$$G_f = 0.308\beta_w\sqrt{f_t} \tag{18}$$

$$\tau_f = 1.5\beta_w f_t \tag{19}$$

$$\beta_w = \sqrt{\frac{2 - w_f/(s_f \sin\beta)}{1 + w_f/(s_f \sin\beta)}} \tag{20}$$

$$f_t = 0.395 f_{cu}^{0.55} \tag{21}$$

In Eqs. (8)-(21), L_m is the maximum mobilized bond length in the fibre direction from the critical shear crack to the softening front (see Fig 5); h_{db} is the vertical distance from the crack end to the intersection between the right most debonded FRP strip and the critical shear crack (i.e. point *N* in Fig. 5); h_{df} is the vertical distance from the crack tip to the point of the intersection between the debonding front and the critical shear crack (i.e. point *M* in Fig. 5); $w_{e,p}$ (denoted by $w_{e,p-s}$ and $w_{e,p-u}$ in Fig. 3 for FRP side strips and FRP U-strips respectively) is the crack end width at which the FRP shear contribution (V_f) reaches its peak value $V_{f,p}$ (denoted by $V_{f,p-s}$ and $V_{f,p-u}$ in Fig. 3 for FRP side strips and FRP U-strips respectively); δ_f is the interfacial slip at the shear crack at which the FRP is fully debonded; β_w is the strip width coefficient; G_f and τ_f are the interfacial facture energy and maximum interfacial shear stress respectively, which can be determined according to Lu et al.'s (2005) bond-slip model as shown in Eqs. (18)-(21); f_{cu} is the cube compressive strength of concrete and can be estimated from the cylinder compressive strength of concrete using $f_{cu} = f_c^{'}/0.8$ as may be deduced from EN-BS 1992-1-1 (2004). It should be noted that in deriving the expressions of D_{frp} [i.e. Eqs. (8) and (13)], the following condition representing a reasonable limitation on the practical FRP configuration and/or beam size should be satisfied as explained in Chen et al. (2011): $(h_t + h_{f,e})\text{cosec}\beta > h_b\text{cosec}\beta$ and $(h_t + h_{f,e})\text{cosec}\beta > L_e$.

K_s-w_e Curve

To study the shear interaction between externally bonded FRP strips and internal steel stirrups, an FE model was proposed by Chen et al. (2010) in which appropriate bond-slip relationships were employed to accurately depict the bond behaviour of both FRP strips and steel stirrups. Numerical results from Chen et al. (2010) showed that the mobilization factor K_s of steel stirrups depends mainly on the beam height as well as the diameter ϕ_s and yield strength f_y of steel bars. The concrete strength ($f_c^{'}$) also has some effect on the $K_s - w_e$ curve, but it is rather small within the practical range of $f_c^{'}$ values.

Based on these observations, the following expression for the $K_s - w_e$ curve was developed by curve-fitting based on the numerical results for a concrete strength $f_c^{'} = 30$ MPa (Chen 2010):

$$K_s = \frac{w_e^{1.4}}{A + w_e^{1.4}} \tag{22}$$

where A is a constant reflecting the effects of beam size, steel bar diameter and yield strength. For plain bar stirrups,

$$A = \frac{1.48\left[L_n\left(h_{f,e}\right) - 4.52\right]\left(f_y - 173\right)\left(\phi_s + 0.935\right)}{10000} \tag{23}$$

For deformed bar stirrups,

$$A = \frac{4.94\left[L_n\left(h_{f,e}\right) - 3.34\right]\left(f_y - 245\right)\left(\phi_s - 0.767\right)}{100000} \tag{24}$$

Example comparisons between the predictions of the Eqs. (22)-(24) and the original numerical results are shown in Figs. 6 and 7 respectively for plain and deformed bars. Clearly these expressions are in close agreement with the numerical $K_s - w_e$ curves. It should be noted that although only a limited number of cases are considered in Figs. 6 and 7, this conclusion has been validated against a much larger number of $K_s - w_e$ curves covering practical ranges of beam height, bar diameter, and bar yield strength (Chen 2010).

Shear Interaction Factor (*K*)

The equation for the shear capacity of an RC beam shear strengthened with FRP [i.e. Eq. (2)] may alternatively be expressed as

$$V_u = V_c + V_{s,p} + KV_{f,p} \tag{25}$$

where K is termed the shear interaction factor which reflects the reduction of the efficiency of the FRP strengthening due to the adverse interaction effect between steel stirrups and FRP strips. The term $KV_{f,p}$ in Eq. (25) thus represents the net additional shear resistance contributed by the externally bonded FRP shear reinforcement. Comparing Eq. (2) with Eq. (25) gives:

$$K = K_f + \left(K_s - 1\right)\frac{V_{s,p}}{V_{f,p}} = K_f + \left(K_s - 1\right)\cdot\mu \tag{26}$$

where μ is the ratio of the shear contribution of steel stirrups to that of FRP strips if the effect of shear interaction is not considered:

$$\mu = \frac{V_{s,p}}{V_{f,p}} = \frac{f_y A_{sv}}{f_{f,e} A_{frp}} \tag{27}$$

in which A_{sv} and A_{frp} are respectively the cross-sectional area of the steel stirrups and that of the FRP strips intersected by the critical shear crack. Eq. (26) shows that the efficiency of FRP shear strengthening is affected not only by the mobilization factors K_f and K_s, but also by the cross-sectional area of steel stirrups relative to that of FRP strips as implied by the definition of μ.

For a given strengthening design, μ is known, so the development of K with the crack end width can be found by substituting the expressions of K_s and K_f into Eq. (26). Examples of the $K - w_e$ curve so obtained are shown in Figs. 8(a) and 8(b) respectively for FRP side strips and FRP U-strips. Clearly, an increase in μ results in a decrease in the peak value of K, indicating that the FRP strengthening is less efficient for beams with heavier steel shear reinforcement. This trend is in agreement with test observations (Bousselham and Chaallal 2004; Li et al. 2001; Pellegrino and Modena 2002, 2006).

At the ultimate state, the contribution of steel stirrups and FRP strips combined reaches the maximum value. This is equivalent to K reaching its maximum value $K_{\max}$

on the $K - w_e$ curve as shown in Fig. 8. The $K_{\max}$ value can then be used in Eq. (25) for the ultimate limit state design.

For FRP U-strips, the $K_{\max}$ value usually occurs at a crack end width w_e when V_f peaks (i.e. $w_e = w_{e,p}$), thus, $K_f = K_{f,p} = 1$ [see Fig. 8(b)]. Consequently, the $K_{\max}$ value can be obtained by substituting $K_f = 1$ into Eq. (26) and the corresponding value of w_e (i.e. $w_e = w_{e,p}$) from Eq. (15) (see Fig. 3) into Eq. (22) respectively, as follows:

$$K_{\max} = 1 - \mu \cdot (1 - K_s) \tag{28}$$

in which

$$K_s = \frac{w_{e,p}^{1.4}}{A + w_{e,p}^{1.4}} \tag{29}$$

where A can be obtained from Eqs. (23) and (24) respectively for plain bars and deformed bars, and $w_{e,p}$ from Eq. (15).

For FRP side strips, the crack end width at which $K_{\max}$ occurs, $w_{e,u}$, varies with μ [see Fig. 8(a)]: the larger the μ, the larger the $w_{e,u}$. Finding the $K_{\max}$ value using the $K - w_e$ curve shown in Fig. 8(a) is somewhat involved because it in turn depends on the corresponding $K_f - w_e$ and $K_s - w_e$ curves. To address this problem, the following approximate expression of $K_{\max}$ has been developed based on a regression analysis of a large number of $K_{\max}$ values obtained from the above procedure covering the geometrical and material properties of the FRP strips, steel stirrups and beam over their respective practical ranges (see the specifications below):

$$K_{\max} = \frac{B}{B + \mu} \tag{30}$$

in which

$$B = \frac{1.01 \times 10^5}{\phi_s^{0.834} f_y^{1.88}} (\lambda_h + 2.11) \qquad \text{for plain bar stirrups} \tag{31}$$

and

$$B = \frac{2.05 \times 10^5}{\phi_s^{1.13} f_y^{1.71}} (\lambda_h + 1.58) \qquad \text{for deformed bar stirrups} \tag{32}$$

where $\lambda_h = h_{f,e} / L_e$ is the normalized effective height of FRP on the beam sides. It should be noted that Eqs. (30)-(32) were obtained using the flowing ranges of parameters: for plain bars, $f_y = 250 \sim 450$ MPa, $\phi_s = 6 \sim 10$ mm; for deformed bars, $f_y = 450 \sim 650$ MPa, $\phi_s = 8 \sim 16$ mm; and $\lambda_h = 1 \sim 20$.

Representative comparisons between predictions of Eqs. (30)-(32) and $K_{\max}$ values obtained directly from $K - w_e$ curves are shown in Figs. 9(a) and 9(b) for plain bar stirrups and deformed bar stirrups respectively. Clearly these expressions provide a close approximation to the $K_{\max}$ value for FRP side strips and are adopted in the following analyses.

COMPARISON WITH TEST DATA

To validate the proposed shear strength model, an extensive literature review has been carried out to collect test data of RC beams shear-strengthened with bonded FRP. Table 1

presents the collected database for shear-strengthened RC beams that failed due to FRP debonding. It contains 131 specimens, including 78 beams shear-strengthened with FRP side-strips and 53 beams shear-strengthened with FRP U-strips. Only the geometric and material properties required to determine the contribution of FRP strips to the shear capacity of the strengthened beam by the strength model presented in this paper are shown. Further details can be found in the original sources or in Chen (2010). Test results that were not sufficiently well documented, and those specimens damaged before strengthening [e.g. specimen F1 of Mitsui et al. (1998)], with a very low concrete strength ($f_c^{'}$ <15 MPa) [some specimens of Monti and Liotta (2007)] or having a marginal FRP shear enhancement [e.g. specimen V4 of Sundarraja et al. (2008)], have been excluded from the database. The test data listed in Table 1 have the following parametric ranges: beam height $h = 110 - 600$ mm; web thickness $b_w = 70 - 300$ mm; cylinder compressive strength of concrete $f_c^{'} = 20.5 - 71.4$ MPa; and steel shear reinforcement ratio $\rho_s = 0.0 - 0.75\%$. Most of these specimens have a shear span-to-depth ratio $s/d \geq 2.2$; a few test specimens with $s/d < 2.2$ [e.g. some specimens of Mitsui et al. (1998) with $s/d < 2.2$] are also included in the test database because the FRP debonding failure mode was clearly observed in these specimens. It shall be noted that in Table 1, if the strengthened specimen has a different concrete strength from that of the control specimen, the test shear contribution of the FRP has been adjusted using the method described by Chen and Teng (2003a).

The new shear strength model presented in this paper, as well as the three shear strength model adopted by the recent design guidelines are compared with the collected test data: a) the Australian guideline HB 305 (2008) which adopts Chen and Teng's (2003b) model; b) ACI.440.2R (2008) which adopts Khalifa et al.'s (1998) model; and c) the Italian guideline CNR-DT200 (2004) which adopts Monti and Liotta's (2007) model. As noted by many researchers (Chen and Teng 2003a, b; Khalifa et al. 1998; Monti and Liotta 2007; Triantafillou 1998; Triantafillou and Antonopoulos 2000), the shear crack angle has a significant effect on the FRP shear capacity [also see Eq. (5)]. Given the significant effect of the shear crack angle, the evaluations presented below are in two steps.

In step one, only those specimens with the experimental shear crack angle information (pictures, sketches or text descriptions) in the original sources (which include 74 specimens: 46 with FRP side strips and 28 with FRR U-strips) are used to evaluate the performance of the models mentioned above. The results are shown in Figs. 10(a)-10(d) and Figs. 11(a)-11(d) for the proposed model and the models in HB 305 (2008), ACI.440.2R (2008) and CNR-DT200 (2004), respectively. The coefficient of determination (R^2) is shown in the respective figure for each case. Other statistical characteristics are presented in Table 2. It should be noted that for each of these shear strength models, two comparisons are made: one with the effect of shear interaction neglected (Fig. 10), and the other with the effect of shear interaction included (Fig. 11). It should also be noted that these comparisons are made between the predictive models and the test results, so all partial safety factors for design use have not been included.

Figure 10 clearly shows that if the effect of shear interaction is not considered, the performance of the proposed model in predicting experimental results is similar to that of the model in HB 305 (2008). Both models provide significantly better predictions than the other two models in terms of the coefficient of determination (R^2) and other statistical measures (see Table 2). In particular, it is of interest to note that three of the four models [i.e. except the CNR-DT200 (2004) model] predict an average value of the predicted-to-experimental ratio (referred to as the average ratio hereafter) quite close to

1.0. The same conclusion can be drawn if the predictions for FRP side strips and FRP U-strips are separately assessed (Table 2).

The predictions of the CNR-DT200 (2004) model have a very low average ratio of 0.52 for FRP side strips but a high value of 1.26 for FRP U-strips, indicating that it significantly underestimates the FRP shear contribution (V_f) for FRP side strips but overestimates V_f for FRP U-strips. The significant underestimation of V_f for FRP side strips is chiefly due to the neglect of the FRP bond length above the crack tip and that below the crack end of the effective shear crack as explained in detail by Chen (2010). For FRP U-strips, the overestimation of V_f is caused by the following reasons according to analyses detailed in Chen (2010). First, unlike the HB 305 (2008) model and the proposed model, the CNR-DT200 (2004) model does not specify an upper bound to the FRP maximum stress. As a result, the FRP shear contribution may be overestimated if the FRP material has a very low strength f_f [e.g. for specimen "IIGu" in Malek and Saadatmanesh (1998)]. Second, the model uses $0.9d$ to determine the FRP area contributing to the shear capacity (where d is the effective depth of the RC beam) regardless of the actual bond length of FRP. This may overestimate the FRP shear contribution if the FRP U-strips are bonded to only part of the beam height [e.g. specimens in Khalifa and Nanni (2000)]. Third and more importantly, the expression for the FRP shear contribution in CNR-DT200 (2004) is the FRP force in the fiber direction and it is only valid when the fiber orientation is vertical ($\beta = 90^o$); for other fiber orientations, the expression is incorrect and may lead to unsafe results [e.g. specimen of Hutchinson and Rizkalla (1999)].

Fig. 11 shows that if the effect of shear interaction is considered, the proposed model and the HB 305 (2008) model also perform better than the two other models in terms of R^2; similar conclusions can be drawn if FRP side strips and FRP U-strips are assessed separately as shown in Chen (2010). If other statistical indexes are assessed (Table 2), the Chen and Teng (2003b) model in HB 305 (2008) is slightly more accurate in predicting experimental observations than the proposed model in terms of the coefficient of variation. Both models provide better predictions than the other two models [ACI.440.2R (2008) and CNR-DT200 (2004)].

By comparing Fig. 10 with with Fig. 11, it is clear that considering the effect of shear interaction significantly improves the performance of all four models. The same conclusion can be drawn from the statistical indexes in Table 2.

In step two, the shear crack angle is set to be 45^o for all specimens in the database as is done in most design guidelines [e.g. ACI 440.2R (2008)]. The comparisons on the basis of this assumption are shown in Figs. 12 and 13, with the corresponding statistical information shown in brackets in Table 2. The assumption leads to much more conservative predictions for all the models as expected (see Figs. 12 and 13 and Table 2). Again, it can be seen from the statistics in Table 2 that the proposed model and Chen and Teng's (2003b) model provide the best predictions with the proposed model being slightly better, and that considering the effect of shear interaction significantly improves the performance of all four models.

DESIGN RECOMMENDATION

From the above assessments, it can be seen that although the proposed model is developed upon a more rigorous basis and provides the best performance in predicting the shear contribution of FRP to the shear resistance of the beam when the shear crack angle is set to 45^o, Chen and Teng's (2003b) model as adopted in HB 305 (2008) is still capable of providing satisfactory predictions, particularly when the effect of shear

interaction is considered using the shear interaction factor (K_{max}) proposed in this study. In addition, Chen and Teng's (2003b) model has a simpler form compared with the proposed model; thus, it is more suitable for design use.

For FRP side strips, Eqs. (30)-(32) can be employed to consider the effect of shear interaction.

For FRP U-strips, in general, Eqs. (28) and (29) can be employed to consider the effect of shear interaction. However, the effect of shear interaction is limited if $w_{e,p}$ is larger than a certain value, and can be neglected. For example, when $w_{e,p} \geq 3.0$ mm [which eventually leads to a limitation on $\lambda_h = h_{f,e}/L_e$ according to Eq. (15) for a certain FRP configuration (i.e. w_f, s_f and β) and certain values of $f_c^{'}, \theta$), it can be inferred from Eq. (26) that $K_{\max}$ is usually larger than 0.9 as K_s is normally larger than 0.9 (see Figs. 6 and 7 for reference) and $K_f = 1$ in this case, subject to $\mu = V_s/V_f \leq 1$.

CONCLUDING REMARKS

Built upon the authors' previous work as presented in Chen et al. (2010) and Chen et al. (2011), this paper has presented a shear strength model for the FRP debonding failure mode for RC beams shear-strengthened with FRP strips. A salient feature of the new model is that it takes into account the process of debonding failure (see Chen et al. 2011) and the effect of shear interaction between externally bonded FRP strips and internal steel stirrups (Chen et al. 2010). The new model has been shown to perform well in predicting the shear contribution of FRP by comparing its predictions with a large test database.

Performance comparisons between the new shear strength model and three other shear strength models adopted in existing design guidelines have also been undertaken. These comparisons indicate that the new model has the best performance among the four models examined, and the inclusion of the effect of shear interaction leads to a significant improvement to the performance of all four models. The results have also revealed that the model in ACI.440.2R (2008) shows unsatisfactory performance probably due to its empirical nature and the use of an inappropriate model for the effective FRP bond length; the model in CNR-DT200 (2004) generally provides conservative predictions for FRP side strips but overestimates the shear resistance offered by FRP U-strips. A design recommendation has been proposed based on these comparisons.

It should be noted that the new shear strength model is based on two assumptions: (a) the FRP debonding failure process is dominated by the widening of a single critical shear crack; (b) the critical shear crack governing the FRP debonding process has a linear crack shape. In real RC beams shear-strengthened with FRP strips, secondary shear cracks may exist, and they can have a significant effect. The actual width variation of the critical shear crack is complex and depends on many factors including the amounts of steel and FRP shear reinforcements and steel tension reinforcement. The effects of these two assumptions should be examined in future research.

ACKNOWLEDGEMENTS

The authors are grateful for the financial support received from the Research Grants Council of the Hong Kong Special Administrative Region (Project No: PolyU 5151/03E),

the Niche Area Funding Scheme of The Hong Kong Polytechnic University, and National Natural Science Foundation of China (Project No: 51108097). They would also like to acknowledge the support from the Scottish Funding Council for the Joint Research Institute between the University of Edinburgh and Heriot-Watt University which forms part of the Edinburgh Research Partnership in Engineering and Mathematics (ERPem). The authors are also grateful for the following researchers for their valuable help in establishing the database presented in this paper: Drs J.A.O. Barros, L. De Lorenzis, A.J. Beber, G. Kim, H. Oh, G. Gas and Professor Z.F. Chen.

REFERENCES

ACI-440.2R (2008). "Guide for the Design and Construction of Externally Bonded FRP Systems for Strengthening Concrete Structures." American Concrete Institute, Farmington Hills, Michigan, USA.

Adhikary, B. B., and Mutsuyoshi, H. (2004). "Behavior of concrete beams strengthened in shear with carbon-fiber sheets." *J. Compos. Constr.*, 8(3), 258-264.

Ali, M. S. M., Oehlers, D. J., and Seracino, R. (2006). "Vertical shear interaction model between external FRP transverse plates and internal steel stirrups." *Eng. Struct.*, 28(3), 381-389.

Alsulaikmani, G. J., Sharif, A., Basunbul, I. A., Baluch, M. H., and Ghaleb, B. N. (1994). "Shear repair for reinforced-concrete by fiberglass plate bonding." *ACI Struct. J.*, 91(4), 458-464.

Bank, L. C. (2006). "Composites for Construction: Structural Design with FRP Materials." John Wiley and Sons, Chichester, West Sussex, UK.

Barros, J. A. O., and Dias, S. J. E. (2006). "Near surface mounted CFRP laminates for shear strengthening of concrete beams." *Cem. Concr. Compos.*, 28(3), 276-292.

Beber, A. J., and Campos Filho, A. (2005). "CFRP composites on the shear strengthening of reinforced concrete beams." *IBRACON Structural Journal*, 1(2), 127-143.

Bousselham, A., and Chaallal, O. (2004). "Shear strengthening reinforced concrete beams with fiber-reinforced polymer: Assessment of influencing parameters and required research." *ACI Struct. J.*, 101(2), 219-227.

Bousselham, A., and Chaallal, O. (2008). "Mechanisms of shear resistance of concrete beams strengthened in shear with externally bonded FRP." *J. Compos. Constr.*, 12(5), 499-512.

BS-EN-992-1-1 (2004). "Eurocode 2: Design of Concrete Structures — Part 1-1: General Rules and Rules for Buildings." British Standards Institute (BSI), BSI Group Headquarters 389 Chiswick High Road, London W4 4AL, UK.

Carolin, A., and Taljsten, B. (2005). "Experimental study of strengthening for increased shear bearing capacity." *J. Compos. Constr.*, 9(6), 488-496.

Chaallal, O., Nollet, M.-J., and Perraton, D. (1998). "Strengthening of RC beams by externally bonded side CFRP strips." *J. Compos. Constr.*, 2(2), 111-113.

Chen, G. M. (2010). "Shear Behaviour and Strength of RC Beams Shear-Strengthened with Externally Bonded FRP Reinforcement." PhD, The Hong Kong Polytechnic University, Hong Kong, China.

Chen, G. M., Teng, J. G., and Chen, J. F. (2011). "Process of debonding in RC beams shear-strengthened with FRP U-strips or side strips." *Int. J. Solids Struct.*, Under review.

Chen, G. M., Teng, J. G., Chen, J. F., and Rosenboom, O. A. (2010). "Interaction between Steel Stirrups and Shear-Strengthening FRP Strips in RC Beams." *J. Compos. Constr.*, 14(5), 498-509.

Chen, J. F., and Teng, J. G. (2003a). "Shear capacity of fiber-reinforced polymer-strengthened reinforced concrete beams: Fiber reinforced polymer rupture." *J. Struct. Eng.-ASCE*, 129(5), 615-625.

Chen, J. F., and Teng, J. G. (2003b). "Shear capacity of FRP-strengthened RC beams: FRP debonding." *Constr. Build. Mater.*, 17(1), 27-41.

CNR-DT200 (2004). "Guide for the Design and Construction of Externally Bonded FRP Systems for Strengthening Existing Structures." Advisory Committee on Technical Recommendations for Construction, National Research Council, Rome, Italy.

Deniaud, C., and Cheng, J. J. R. (2001). "Sheer behavior of reinforced concrete T-beams with externally bonded fiber-reinforced polymer sheets." *ACI Struct. J.*, 98(3), 386-394.

Diagana, C., Li, A., Gedalia, B., and Delmas, Y. (2003). "Shear strengthening

effectiveness with CFF strips." *Eng. Struct.*, 25(4), 507-516.
Dias, S. J. E., and Barros, J. A. O. (2010). "Performance of reinforced concrete T beams strengthened in shear with NSM CFRP laminates." *Eng. Struct.*, 32(2), 373-384.
Feng, X. S., Li, J., and Chen, Z. F. (2004). "Experimental research on shear strengthening of reinforced concrete beams with externally bonded CFRP sheets." *Proceedings of the Third International Conference on Earthquake Engineering - New Frontier and Research Transformation*, W. Q. Liu, F. G. Yuan, and P. C. Chang, eds., Intellectual Property Publ House & China Waterpower Press, Beijing, 436-440.
fib (2001). "Externally Bonded FRP Reinforcement for RC Structures." Federation Internationale du Beton (fib), Lausanne, Switzerland.
Grande, E., Imbimbo, M., and Rasulo, A. (2009). "Effect of Transverse Steel on the Response of RC Beams Strengthened in Shear by FRP: Experimental Study." *J. Compos. Constr.*, 13(5), 405-414.
HB305 (2008). "Design Handbook for RC Structures Retrofitted with FRP and Metal Plates: Beams and Slabs." Standards Australia, GPO Box 476, Sydney, NSW, Australia.
Hollaway, L. C., and Teng, J. G. (2008). "Strengthening and Rehabilitation of Civil Infrastructures Using Fibre-reinforced Polymer (FRP) Composites." Woodhead Publishing Limited, Cambridge England.
Hutchinson, R. L., and Rizkalla, S. H. (1999). "Shear strengthening of AASHTO bridge girders using carbon fibre reinforced polymer sheets." *Proc., The Fourth International Symposium on Fibre Reinforced Polymer Reinforcement for Reinforcement Concrete Structures* ACI Publications SP-188, 945-956.
Kachlakev, D. I., and Barnes, W. A. (1999). "Flexural and shear performance of concrete beams strengthened with fibre reinforced polymer laminates." *Proc., The Fourth International Symposium on Fibre Reinforced Polymer Reinforcement for Reinforced Concrete Structures*, ACI Publications SP-188, 959-971.
Kage, T., Abe, M., Lee, H. S., and Tomosawa, F. (1997). "Effect of CFRP sheets on shear strengthening of RC beams damaged by corrosion of stirrup." *Proc., Third International Symposium on Non-Metallic (FRP) Reinforcement for Concrete Structures*, 443-450.
Khalifa, A., Gold, W. J., Nanni, A., and Abel-Aziz, M. I. (1998). "Contribution of externally bonded FRP to shear capacity of RC flexural members." *J. Compos. Constr.*, 2(4), 195-202.
Khalifa, A., and Nanni, A. (2000). "Improving shear capacity of existing RC T-section beams using CFRP composites." *Cem. Concr. Compos.*, 22(3), 165-174.
Khalifa, A., and Nanni, A. (2002). "Rehabilitation of rectangular simply supported RC beams with shear deficiencies using CFRP composites." *Constr. Build. Mater.*, 16(3), 135-146.
Khalifa, A., Tumialan, G., Nanni, A., and Belarbi, A. (1999). "Shear strengthening of continuous reinforced concrete beams using externally bonded carbon fibre reinforced polymer sheets." *Proc., The Fourth International Symposium on Fibre Reinforced Polymer Reinforcement for Reinforcement Concrete Structures.*, ACI Publications SP-188, 995-1008.
Kim, G., Sim, J., and Oh, H. (2008). "Shear strength of strengthened RC beams with FRPs in shear." *Constr. Build. Mater.*, 22(6), 1261-1270.
Li, A., Diagana, C., and Delmas, Y. (2001). "CRFP contribution to shear capacity of strengthened RC beams." *Eng. Struct.*, 23(10), 1212-1220.
Li, A., Diagana, C., and Delmas, Y. (2002). "Shear strengthening effect by bonded composite fabrics on RC beams." *Compos. Pt. B-Eng.*, 33(3), 225-239.
Malek, A. M., and Saadatmanesh, H. (1998). "Analytical study of reinforced concrete beams strengthened with web-bonded fiber reinforced plastic plates or fabrics." *ACI*

Struct. J., 95(3), 343-352.
Matthys, S. (2000). "Structural Behaviour and Design of Concrete Members Strengthened with Externally Bonded FRP Reinforcement." PhD, University of Ghent, Belgium, Ghent.
Mitsui, Y., Murakami, K., Takeda, K., and Sakai, H. (1998). "A study on shear reinforcement of reinforced concrete beams externally bonded with carbon fiber sheets." *Compos. Interfaces*, 5(4), 285-295.
Mofidi, A., and Chaallal, O. (2011). "Shear Strengthening of RC Beams with EB FRP: Influencing Factors and Conceptual Debonding Model." *J. Compos. Constr.*, 15(1), 62-74.
Monti, G., and Liotta, M. (2007). "Tests and design equations for FRP-strengthening in shear." *Constr. Build. Mater.*, 21(4), 799-809.
Oehlers, D. J., and Seracino, R. (2004). "Design of FRP and Steel Plated RC structures: Retrofitting Beams and Slabs for Strength, Stiffness and Ductility." Elsevier, UK.
Park, S. Y., Namaan, A. E., Lopez, M. M., and Till, R. D. (2001). "Shear strengthening effect of RC beams using glued CFRP sheets." *Proc., The International Conference on FRP Composites in Civil Engineering*, 669-676.
Pellegrino, C., and Modena, C. (2002). "Fiber reinforced polymer shear strengthening of reinforced concrete beams with transverse steel reinforcement." *J. Compos. Constr.*, 6(2), 104-111.
Pellegrino, C., and Modena, C. (2006). "Fiber-reinforced polymer shear strengthening of reinforced concrete beams: Experimental study and analytical modeling." *ACI Struct. J.*, 103(5), 720-728.
Pellegrino, C., and Modena, C. (2008). "An experimentally based analytical model for the shear capacity of FRP-strengthened reinforced concrete beams." *Mech. Compos. Mater.*, 44(3), 231-244.
Rizzo, A., and De Lorenzis, L. (2009). "Behavior and capacity of RC beams strengthened in shear with NSM FRP reinforcement." *Constr. Build. Mater.*, 23(4), 1555-1567.
Sato, Y., Ueda, T., Kakuta, Y., and Ono, S. (1997). "Ultimate shear capacity of reinforced concrete beams with carbon fibre sheet." *Proc., Third Symposium on Non-Metallic (FRP) Reinforcement for Concrete Structures*, 499–505.
Sato, Y., Ueda, T., Kakuta, Y., and Tanaka, T. (1996). "Shear reinforcing effect of carbon fibre sheet attached to side of reinforced concrete beams." *Proc., Advanced Composite Materials in Bridges and Structures*, 621-627.
Sundarraja, M. C., Rajamohan, S., and Bhaskar, D. (2008). "Shear strengthening of RC beams using GFRP vertical strips - An experimental study." *J. Reinf. Plast. Compos.*, 27(14), 1477-1495.
Taljsten, B. (2003). "Strengthening concrete beams for shear with CFRP sheets." *Constr. Build. Mater.*, 17(1), 15-26.
Taljsten, B., and Elfgren, L. (2000). "Strengthening concrete beams for shear using CFRP-materials: evaluation of different application methods." *Compos. Pt. B-Eng.*, 31(2), 87-96.
Teng, J. G., and Chen, J. F. (2009). "Mechanics of debonding in FRP-plated RC beams." *Proc. Inst. Civil Eng.-Struct. Build.*, 162(5), 335-345.
Teng, J. G., Chen, J. F., Smith, S. T., and Lam, L. (2002). "FRP-Strengthened RC Structures." John Wiley and Sons, Chichester, West Sussex, UK.
Teng, J. G., Lam, L., and Chen, J. F. (2004). "Shear strengthening of RC beams using FRP composites." *Progress in Structural Engineering and Materials*, 6(3), 173-184.
Triantafillou, T. C. (1998). "Shear strengthening of reinforced concrete beams using

epoxy-bonded FRP composites." *ACI Struct. J.*, 95(2), 107-115.
Triantafillou, T. C., and Antonopoulos, C. P. (2000). "Design of concrete flexural members strengthened in shear with FRP." *J. Compos. Constr.*, 4(4), 198-205.
Uji, K. (1992). "Improving shear capacity of existing reinforced concrete members by applying carbon fibre sheets." *Transaction of the Japan Concete Institute*, 14, 253-266.
Zhang, Z. C., and Hsu, C. T. T. (2005). "Shear strengthening of reinforced concrete beams using carbon-fiber-reinforced polymer laminates." *J. Compos. Constr.*, 9(2), 158-169.

LIST OF TABLES

LIST OF FIGURES

Table 1. Experimental Database for FRP Shear-Strengthened RC beams Failing by FRP Debonding

Reference	Speci.	Beam properties					FRP properties								Steel stirrup properties					Test results		
		f_c' MPa	b_w mm	h mm	d mm	Sect.	Type	Conf.	E_f GPa	t_f mm	f_f MPa	w_f mm	S_f mm	β *deg.*	Type	Φ_s mm	S_s mm	E_s GPa	f_y MPa	θ *deg.*	$V_{u,test}$ kN	$V_{f,test}$ kN
Uji (1992)	5	24.1	100	200	160	R	C	SP90	230	0.097	2454	100	100	90	NA					45	44.6	20.1
	6	26.9	100	200	160	R	C	SP45	230	0.097	2454	100	141.4	45	NA					45	56.8	31.4
	7	26.9	100	200	160	R	C	SP90	230	0.194	2454	100	100	90	NA					45	44.6	19.2
Al-Sulaimani et al. (1994)	SO	37.7	150	150	113	R	C	SS90	16	3	200	20	50	90	D	6	200	200	450	45	41.5	8.2
	SP	37.7	150	150	113	R	C	SS90	16	3	200	20	50	90	D	6	200	200	450	45	41.2	7.9
	WO	37.7	150	150	113	R	C	SP90	16	3	200	20	20	90	D	6	200	200	450	45	42.0	8.7
	WP	37.7	150	150	113	R	C	SP90	16	3	200	20	20	90	D	6	200	200	450	45	45.2	11.9
Sato et al. (1996)	S2	45.2	200	300	260	R	C	SS90	230	0.11	3480	30	60	90	NA					28	160.5	68.4
	S4	37.5	200	300	260	R	C	SP90	230	0.11	3480	30	30	90	NA					28	156.3	64.2
Kage et al. (1997)	SB1310	39.2	200	200	160	R	C	SP90	284.2	0.097	3430	100	100	90	R	3	100	178.36	132.3	45	84.7	31.1
	SB1210	39.2	200	200	160	R	C	SP90	284.2	0.097	3430	100	100	90	R	3	100	178.36	132.3	45	79.0	22.1
	SB1214	39.2	200	200	160	R	C	SP90	284.2	0.097	3430	100	100	90	R	3	100	178.36	132.3	45	78.2	24.7
	SB1218	39.2	200	200	160	R	C	SP90	284.2	0.097	3430	100	100	90	R	3	100	178.36	132.3	45	79.2	25.6
Chaallal et al. (1998)	RS90	35	150	250	210	R	C	SS90	150	1	2400	50	100	90	D	6	200	200	400	45	91.3	34.3
	RS135	35	150	250	210	R	C	SS45	150	1	2400	50	150	45	D	6	200	200	400	45	96.8	43.5
Mitsui et al. (1998)	A1	28.5	150	250	220	R	C	SP90	230	0.167	3430	50	50	90	NA					40	134.4	40.2
	B1	28.5	150	250	220	R	C	SP90	230	0.167	3430	50	50	90	NA					40	137.3	43.2
	C1	28.5	150	250	220	R	C	SP90	230	0.167	3430	50	50	90	NA					40	128.5	34.3
	D1	28.5	150	250	220	R	C	SP90	230	0.167	3430	50	50	90	NA					40	126.5	55.4
	E1	28.5	150	250	220	R	C	SP90	230	0.167	3430	50	50	90	NA					40	108.9	37.8
Triantafillou (1998)	S1a	30	70	110	100	R	C	SS90	235	0.11	3300	30	45	90	NA					20	43.5	*27.1*
	S1b	30	70	110	100	R	C	SS90	235	0.11	3300	30	45	90	NA					20	38.9	*22.5*
	S1(45)	30	70	110	100	R	C	SS45	235	0.11	3300	30	63.63	45	NA					20	44.5	*28.1*
	S2a	30	70	110	100	R	C	SS90	235	0.11	3300	30	30	90	NA					20	48.1	*31.7*
	S2b	30	70	110	100	R	C	SS90	235	0.11	3300	30	30	90	NA					20	42.2	*25.8*
	S2(45)	30	70	110	100	R	C	SS45	235	0.11	3300	30	42.42	45	NA					20	47.3	*30.9*
	S3a	30	70	110	100	R	C	SS90	235	0.147	3300	30	30	90	NA					20	42.8	*26.4*
	S3b	30	70	110	100	R	C	SS90	235	0.147	3300	30	30	90	NA					20	37.5	*21.1*
	S3(45)	30	70	110	100	R	C	SS45	235	0.147	3300	30	42.42	45	NA					20	40.7	*24.3*
Kachlakev and Barnes (1999)	C1, 2L	27.5	152	152	101	R	C	SP90	230	0.222	3400	50	50	90	NA					25	114.0	*19.1*
	C1, 3L	27.5	152	152	101	R	C	SP90	230	0.333	3400	50	50	90	NA					25	100.6	*18.2*
	C2, 3L	27.5	152	152	101	R	C	SP90	230	0.33	3400	50	50	90	NA					25	84.8	*34.1*
Taljsten and Elfgren(2000)	SR1	53.8	180	500	460	R	C	SS45	70.8	0.8	860	300	848.5	45	NA					45	195.0	*89.0*
	SR2	52.7	180	500	460	R	C	SP45	70.8	0.8	860	1	1.414	45	NA					45	243.0	*122.5*
Ref.[1]	*BT5*	*35*	*150*	*405*	*360*	*T*	*C*	*SS90*	*228*	*0.165*	*3790*	*50*	*125*	*90*	*NA*					*45*	*121.5*	*31.5*

Table 1. (Continued.)

Reference	Speci.	Beam properties					FRP properties								Steel stirrup properties						Test results		
		f_c' MPa	b_w mm	h mm	d mm	Sect.	Type	Conf.	E_f GPa	t_f mm	f_f MPa	w_f mm	S_f mm	β *deg.*	Type	Φ_s mm	S_s mm	E_s GPa	f_y MPa	θ *deg.*	$V_{u,test}$ kN	$V_{f,test}$ kN
Park et al. (2001)	3	25.4	100	250	200	R	C	SS90	178.6	1.2	2868	25	75	90	NA					40	44.1	18.2
	5	25.4	100	300	250	T	C	SS90	178.6	1.2	2868	25	75	90	D	6	75	200	325	30	107.3	25.2
Pellegrino and Modena (2002)	TR30C2	27.5	150	300	250	R	C	SP90	233.6	0.165	3550	1	1	90	D	8	200	210	548	45	120.0	45.3
	TR30C3	27.5	150	300	250	R	C	SP90	233.6	0.495	3550	1	1	90	D	8	200	210	548	45	112.8	38.1
	TR30C4	27.5	150	300	250	R	C	SP90	233.6	0.495	3550	1	1	90	D	8	200	210	548	45	140.2	65.5
	TR30D1	31.4	150	300	250	R	C	SP90	233.6	0.33	3550	1	1	90	D	8	200	210	548	45	193.0	31.5
	TR30D2	31.4	150	300	250	R	C	SP90	233.6	0.495	3550	1	1	90	D	8	200	210	548	45	213.3	51.8
	TR30D2	31.4	150	300	250	R	C	SP90	233.6	0.495	3550	1	1	90	D	8	200	210	548	45	247.5	86.0
	TR30D4	31.4	150	300	250	R	C	SP90	233.6	0.33	3550	1	1	90	D	8	200	210	548	45	208.8	47.3
	TR30D4	31.4	150	300	250	R	C	SP90	233.6	0.33	3550	1	1	90	D	8	200	210	548	45	212.0	50.5
Taljsten (2003)	RC1	67.4	180	500	465	R	C	SP45	234	0.11	4500	1	1.414	45	NA					35	306.1	182.0
	C1	67.4	180	500	465	R	C	SP45	234	0.07	4500	1	1.414	45	NA					31	246.7	122.6
	C2	71.4	180	500	465	R	C	SP45	234	0.11	4500	1	1.414	45	NA					32	257.2	133.2
	C3	58.7	180	500	465	R	C	SP90	234	0.11	4500	1	1	90	NA					30	260.6	136.6
	C5	71.4	180	500	465	R	C	SP45	234	0.165	4500	1	1.414	45	NA					33	334.3	210.6
Beber and Campos Filho (2005)	V9_A	32.8	150	300	261	R	C	SS90	230	0.111	3400	50	100	90	NA					19.5	196.2	82.4
	V9_B	32.8	150	300	261	R	C	SS90	230	0.111	3400	50	100	90	NA					19.5	208.6	94.7
	V21_A	32.8	150	300	261	R	C	SS90	230	0.111	3400	50	100	90	NA					19.5	230.4	116.5
	V12_B	32.8	150	300	261	R	C	SS45	230	0.111	3400	50	141.4	45	NA					19.5	203.3	89.5
	V14_B	32.8	150	300	261	R	C	SS45	230	0.111	3400	50	141.4	45	NA					19.5	183.3	69.5
	V13_A	32.8	150	300	261	R	C	SP90	230	0.111	3400	1	1	90	NA					19	244.0	*130.2*
	V13_B	32.8	150	300	261	R	C	SP90	230	0.111	3400	1	1	90	NA					19	251.5	*137.7*
	V14_A	32.8	150	300	261	R	C	SP45	230	0.111	3400	1	1.414	45	NA					15	256.8	*142.9*
	V15_A	32.8	150	300	261	R	C	SP45	230	0.111	3400	1	1.414	45	NA					15	241.1	*127.3*
	V20_B	32.8	150	300	261	R	C	SS90	205	1.4	2500	50	100	90	NA					19	285.8	*172.0*
	V22_B	32.8	150	300	261	R	C	SS90	205	1.4	2500	50	100	90	NA					19	225.0	*111.2*
	V21_B	32.8	150	300	261	R	C	SS45	205	1.4	2500	50	141.4	45	NA					19	271.4	*157.6*
	V22_A	32.8	150	300	261	R	C	SS45	205	1.4	2500	50	141.4	45	NA					19	251.2	*137.4*
Zhang and Hsu (2005)	Z4-90	43.8	152.	228.	188	R	C	SS90	165	1.2	2800	40	127	90	NA					45	73.7	*27.6*
	Z4-45	43.8	152.	228.	188	R	C	SS45	165	1.2	2800	40	127	45	NA					45	82.2	*36.7*
	Z6-90	43.8	152.	228.	188	R	C	SS90	165	1.2	2800	40	127	90	NA					45	63.9	*21.0*
Corolin and Taljsten (2005)	290a	46.6	180	500	435	R	C	SP90	234	0.11	4500	1	1	90	NA					30	256.0	*134.0*
	290b	41.0	180	500	435	R	C	SP90	234	0.11	4500	1	1	90	NA					25	298.0	*181.0*
	345	56.0	180	500	435	R	C	SP45	234	0.17	4500	1	1.414	45	NA					25	334.0	*204.0*
	290	*36.3*	*180*	*400*	*335*	*R*	*C*	*SP90*	*234*	*0.11*	*4500*	*1*	*1*	*90*	*D*	*6*	*200*	*210*	*515*	*45*	*298.0*	*61.0*

Table 1. (Continued.)

Reference	Speci.	Beam properties					FRP properties								Steel stirrup properties					Test results		
		f_c' MPa	b_w mm	h mm	d mm	Sect.	Type	Conf.	E_f GPa	t_f mm	f_f MPa	w_f mm	S_f mm	β *deg.*	Type	Φ_s mm	S_s mm	E_s GPa	f_y MPa	θ *deg.*	$V_{u,test}$ kN	$V_{f,test}$ kN
Ref.[2]	390	36.3	180	400	335	R	C	SP90	234	0.17	4500	1	1	90	D	6	200	210	515	45	298.0	61.0
Ref.[3]	V5	29.1	100	150	120	R	G	SS90	73	1	3400	40	45	90	NA					45	29.5	13.5
Kim et al. (2008)	CP2-1D	34.7	250	250	220	R	C	SS45	158	1.2	3160	50	100	45	NA					45	178.0	73.0
	CP3-1V	34.7	250	250	220	R	C	SS90	158	1.2	3160	50	100	90	NA					45	95.5	33.0
Grande and Rasulo (2009)	RS2Sa	21	250	450	410	R	C	SP90	392	0.191	2600	1	1	90	D	8	200	210	476	55	240.0	25.0
	RS3Sa	21	250	450	410	R	C	SP90	392	0.191	2600	1	1	90	D	8	300	210	476	42	205.0	45.0
	RS3Sb	21	250	450	410	R	C	SP90	392	0.191	2600	1	1	90	D	8	300	210	476	48	220.0	60.0
	RS4Sb	21	250	450	410	R	C	SP90	392	0.191	2600	1	1	90	D	8	400	210	476	48	180.0	55.0
Sato et al. (1996)	S3	41.3	200	300	260	R	C	US90	230	0.11	3480	30	60	90	NA		120	197	390	28	202.1	110.0
	S5	39.7	200	300	260	R	C	UP90	230	0.11	3480	1	1	90	NA		120	197	390	28	198.2	106.1
Ref.[4]	No.2	35.7	150	300	232	T	C	UP90	230	0.111	3480	1	1	90	R	6	100	183	387	46	223.0	24.0
Ref.[5]	IIGu	36.5	127	203	165	R	C	UP45	200	1.68	105	1	1.414	45	R	6	206	200	420	35	100.8	49.3
Khalifa et al. (1999)	CO2	20.5	150	305	264	R	C	US90	228	0.165	3500	50	125	90	NA		125	200	350	35	88.0	40.0
	CO3	20.5	150	305	264	R	C	UP90	228	0.165	3500	50	50	90	NA		125	200	350	35	113.0	65.0
Ref.[6]	S-Di-CL	59	70	475	410	I	C	US45	230	0.11	3400	50	150	45	D	5.5	300	200	640	30	272.0	62.5
Khalifa and Nanni (2000)	BT2	35	150	405	360	T	C	UP90	228	0.165	3970	1	1	90	NA					45	155.0	65.0
	BT3	35	150	405	360	T	C	UP90	228	0.165	3970	1	1	90	NA					45	157.5	67.5
	BT4	35	150	405	360	T	C	US90	228	0.165	3970	50	125	90	NA					30	162.0	72.0
Ref.[7]	BS5	36	200	450	390	R	C	US90	233	0.111	3500	50	400	90	D	6	400	200	590	29.4	170.0	33.4
Deniaud and Cheng (2001)	T6NS-4	44.1	140	600	520	T	C	US45	230	0.11	3400	50	141.4	45	NA					22	213.6	*103.5*
	T6S4-90	44.1	140	600	520	T	C	US90	230	0.11	3400	50	100	90	R	6	400	200	520	27	272.8	*85.3*
	T6S4-45	44.1	140	600	520	T	G	UP90	17.7	1.8	106	1	1	90	R	6	400	200	520	27	297.5	*109.9*
Khallifa and Nanni (2002)	SO3-2	27.5	150	305	250	R	C	US90	228	0.165	3970	50	125	90	NA					31.4	131.0	*54.0*
	SO4-2	27.5	150	305	250	R	C	US90	228	0.165	3970	50	125	90	NA					31.4	127.5	*62.5*
	SO3-3	27.5	150	305	250	R	C	US90	228	0.165	3970	75	125	90	NA					31.4	133.5	*56.5*
	SO3-4	27.5	150	305	250	R	C	UP90	228	0.165	3970	1	1	90	NA					45	144.5	*67.5*
	SO4-3	27.5	150	305	250	R	C	UP90	228	0.165	3970	1	1	90	NA					30	155.0	*90.0*
Diagana et al. (2003)	PU1	40	130	450	425	R	C	US90	105	0.43	1400	40	200	90	R	6	300	210	240	45	142.5	*32.5*
	PU2	40	130	450	425	R	C	US90	105	0.43	1400	40	250	90	R	6	300	210	240	45	130.0	*20.0*
	PU3	40	130	450	425	R	C	US45	105	0.43	1400	40	300	45	R	6	300	210	240	45	154.5	*44.5*
	PU4	40	130	450	425	R	C	US45	105	0.43	1400	40	350	45	R	6	300	210	240	45	150.0	*40.0*
Adhikary et al. (2004)	C-1	37.2	300	300	245	R	C	UP90	230	0.167	3400	1	1	90	NA					45	165.0	*53.0*
	A-1	*39.6*	*300*	*300*	*245*	*R*	*A*	*UP90*	*120*	*0.286*	*2000*	*1*	*1*	*90*	*NA*					*45*	*155.0*	*43.0*

Table 1. (Continued.)

Reference	Speci.	Beam properties					FRP properties								Steel stirrup properties					Test results		
		f_c' MPa	b_w mm	h mm	d mm	Sect.	Type	Conf.	E_f GPa	t_f mm	f_f MPa	w_f mm	S_f mm	β *deg.*	Type	Φ_s mm	S_s mm	E_s GPa	f_y MPa	θ *deg.*	$V_{u,test}$ kN	$V_{f,test}$ kN
Feng et al. (2004)	SB1-3	32.6	150	360	314	R	C	UP90	235	0.22	4200	1	1	90	R	6	135	205	395	45	240.0	63.5
	SB1-4	32.6	150	360	314	R	C	UP90	235	0.22	4200	1	1	90	R	6	135	205	395	45	253.0	76.5
	SB1-5	32.6	150	360	314	R	C	US90	235	0.22	4200	40	120	90	R	6	135	205	395	45	246.0	69.5
	SB1-6	32.6	150	360	314	R	C	US90	235	0.22	4200	40	120	90	R	6	135	205	395	45	230.0	53.5
	SB1-9	32.6	150	360	314	R	C	US90	235	0.44	4200	40	120	90	R	6	135	205	395	45	240.0	63.5
	SB1-10	32.6	150	360	314	R	C	US90	235	0.44	4200	40	120	90	R	6	135	205	395	45	243.0	66.5
	SB2-3	32.6	150	360	314	R	C	US90	235	0.22	4200	40	120	90	R	6	135	205	395	45	270.0	52.0
	SB3-2	32.6	150	360	314	R	C	US90	235	0.22	4200	40	120	90	R	6	135	205	395	45	310.0	35.0
Beber and Campos Filho (2005)	V10_A	32.8	150	300	261	R	C	US90	230	0.111	3400	50	100	90	NA					25	215.0	82.4
	V10_B	32.8	150	300	261	R	C	US90	230	0.111	3400	50	100	90	NA					25	208.6	94.7
	V17_A	32.8	150	300	261	R	C	US90	230	0.111	3400	50	100	90	NA					25	230.4	116.5
	V11_A	32.8	150	300	261	R	C	US90	230	0.111	3400	50	100	90	NA					25	215.0	101.1
	V11_B	32.8	150	300	261	R	C	US90	230	0.111	3400	50	100	90	NA					25	212.0	98.1
	V17_B	32.8	150	300	261	R	C	US90	230	0.111	3400	50	100	90	NA					25	205.6	91.7
	V19_A	32.8	150	300	261	R	C	US45	230	0.111	3400	50	141.4	45	NA					19	236.8	123.0
	V19_B	32.8	150	300	261	R	C	US45	230	0.111	3400	50	141.4	45	NA					19	230.3	116.4
	V15_B	32.8	150	300	261	R	C	UP90	230	0.111	3400	1	1	90	NA					25	276.7	162.9
	V16_B	32.8	150	300	261	R	C	UP90	230	0.111	3400	1	1	90	NA					25	224.9	111.0
Pellegrino and Modena (2006)	A-U1-C7	41.4	150	300	250	R	C	UP90	230	0.165	3450	1	1	90	D	8	170	200	534	45	238.1	52.9
	A-U2-C-	41.4	150	300	250	R	C	UP90	230	0.33	3450	1	1	90	D	8	170	200	534	45	243.0	57.8
	A-U1-C-	41.4	150	300	250	R	C	UP90	230	0.165	3450	1	1	90	D	8	200	200	534	45	225.0	55.8
	A-U2-C-	41.4	150	300	250	R	C	UP90	230	0.33	3450	1	1	90	D	8	200	200	534	45	229.7	*60.5*
	A-U1-S-	41.4	150	300	250	R	C	UP90	230	0.165	3450	1	1	90	D	8	170	200	534	45	247.3	*49.1*
	A-U1-S-	41.4	150	300	250	R	C	UP90	230	0.165	3450	1	1	90	D	8	200	200	534	45	235.1	*31.7*
Ref.[8]	A12_M	40.2	150	300	280	R	C	US90	390	0.334	3000	25	95	90	NA					45	89.8	*31.5*
Ref.[9]	UW 90	29.3	200	210	173	R	C	UP90	230	0.165	3430	1	1	90	D	6	160	251.5	665.	45	141.5	*19.3*
Dias and Barros(2010)	2S-M(1)	39.7	180	400	360	T	C	US90	218.4	0.176	2863	60	114	90	D	6	300	200	542	60	162.6	*12.8*
	2S-M(2)	*39.7*	*180*	*400*	*360*	*T*	*C*	*US90*	*218.4*	*0.352*	*2863*	*60*	*114*	*90*	*D*	*6*	*300*	*200*	*542*	*60*	*185.1*	*39.8*

Note: Ref.[1]=Khalifa and Nanni (2000); Ref.[2]=Carolin and Taljsten (2005); Ref.[3]=Sundarraja et al. (2008); Ref.[4]=Sato et al. (1997); Ref.[5]=Malek and Saadatmanesh (1998); Ref.[6]=Hutchinson and Rizkalla (1999); Ref.[7]=Matthys (2000); Ref.[8]= Barros and Dias (2006); Ref.[9]=Rizzo and Lorenzis (2009); Section of beam: R=Rectangular section, T=T-section, b_w=web width of beam, h=height of beam, d=effective depth of beam; FRP material: C=CFRP, G=GFRP, A=AFRP, E_f =elastic modulus of FRP, t_f =nominal thickness of FRP, f_f =strength of FRP, w_f =width of FRP in direction perpendicular to fiber direction, s_f =center-to-center spacing of FRP strips in the beam axial direction, β=fiber orientation with respect to beam axis; Speci.=Specimen; Sect.=Section of beam; Conf.=FRP Configurations; deg.=degrees; SSxx=side strips with β=xx^o, SPxx=side sheet with β=xx^o, USxx=U-strips with β=xx^o, UPxx=U-sheet with β=xx^o; Steel stirrups: R=round bars, D=deformed bars, Φ_s=diameter, s_s=spacing, E_s=elastic modulus; f_y =yield strength; f_c'=cylinder compressive strength of concrete; θ=angle of critical shear crack observed in test [assumed to be 45^o if there is no test information except those specimens in the database of Chen and Teng (2003b) for which the crack angles were taken from Chen and Teng (2003b)]; $V_{u,test}$=test shear capacity of beam; $V_{f,test}$=test shear contribution of FRP.

Table 2. Performance of Shear Strength Models (results for a 45^o shear crack angle are listed in brackets)

	Model	Proposed model		HB-305 (2008) model		ACI-440.2R (2008) model		CNR-DT200 (2004)	
Specimens	**Statistics**	$V_{f,pre}/V_{f,test}$	$K_{max}V_{f,pre}/V_{f,test}$	$V_{fpre}/V_{f,test}$	$K_{max}V_{fpre}/V_{f,test}$	$V_{fpre}/V_{f,test}$	$K_{max}V_{fpre}/V_{f,test}$	$V_{f,pre}/V_{f,test}$	$K_{max}V_{fpre}/V_{f,test}$
All	Average	1.01 (0.86)	0.97 (0.77)	1.01 (0.84)	0.96 (.74)	0.89 (0.92)	0.83 (0.79)	0.80 (0.68)	0.75 (0.60)
	SD	0.36 (0.52)	0.29 (0.43)	0.36 (0.52)	0.26 (0.42)	0.80 (0.81)	0.70 (0.63)	0.74 (0.66)	0.61 (0.56)
	CoV (%)	36 (61)	30 (55)	36 (62)	27 (57)	90 (88)	84 (80)	92 (97)	81 (93)
Side-strips	Average	1.05 (0.83)	0.99 (0.74)	1.07 (0.82)	1.01 (0.71)	0.92 (0.92)	0.84 (0.76)	0.52 (0.43)	0.49 (0.37)
	SD	0.40 (0.50)	0.30 (0.37)	0.39 (0.52)	0.25 (0.38)	0.98 (0.90)	0.85 (0.68)	0.43 (0.40)	0.33 (0.31)
	CoV (%)	38 (60)	30 (51)	36 (64)	25 (54)	107 (98)	101 (89)	81 (93)	68 (85)
U-strips	Average	0.96 (0.90)	0.93 (0.83)	0.91 (0.86)	0.88 (0.79)	0.84 (0.93)	0.81 (0.84)	1.26 (1.05)	1.18 (0.95)
	SD	0.30 (0.55)	0.29 (0.49)	0.28 (0.53)	0.27 (0.47)	0.36 (0.66)	0.34 (0.56)	0.90 (0.79)	0.71 (0.66)
	CoV (%)	31 (61)	31 (59)	31 (61)	31 (59)	43 (71)	42 (67)	72 (75)	61 (69)

Note: SD=standard deviation; CoV=coefficient of variation; K_{max} =maximum value of the shear interaction factor (K); $V_{f,pre}$ =FRP shear contribution predicted by a strength model; V_{test}= test value

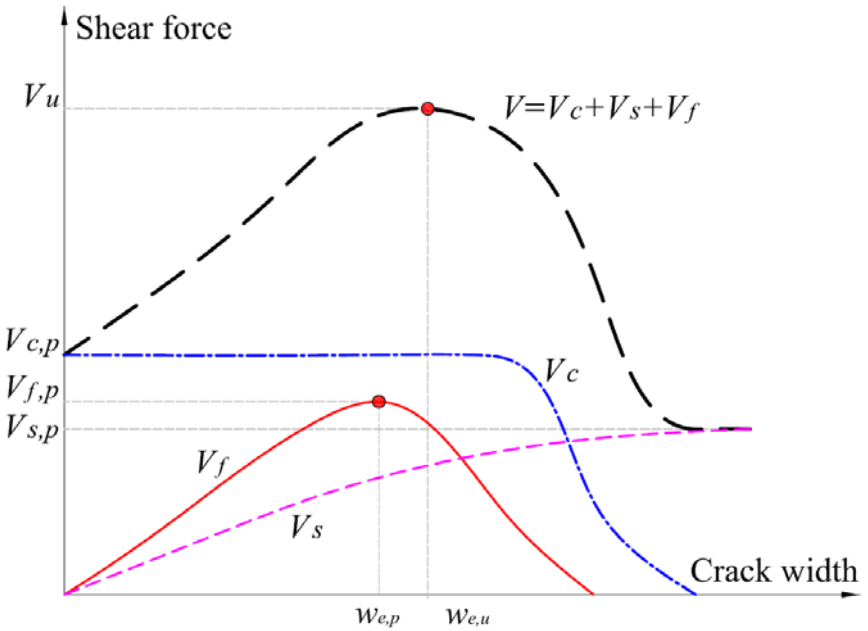

Fig. 1. Development of different components of shear resistance with the crack end width of the critical shear crack

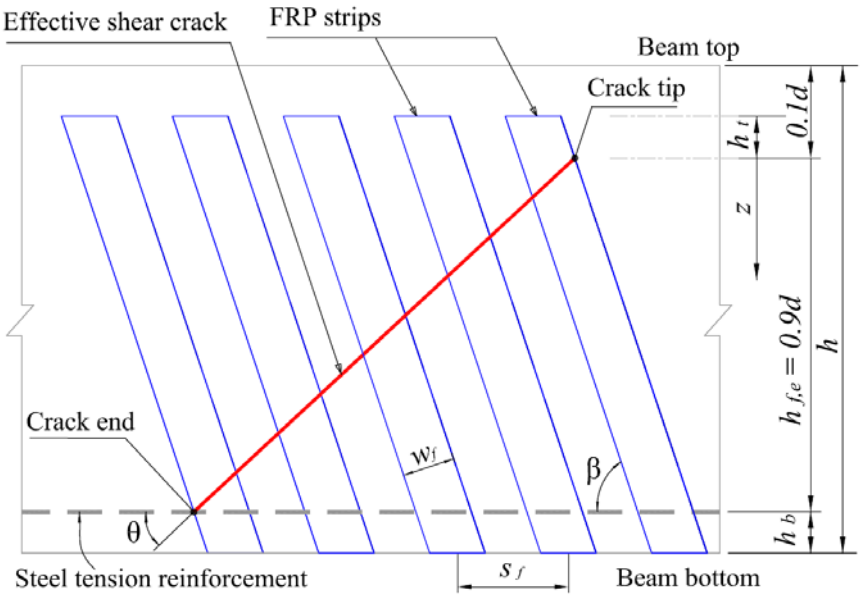

Fig. 2. Notation for a general shear strengthening scheme

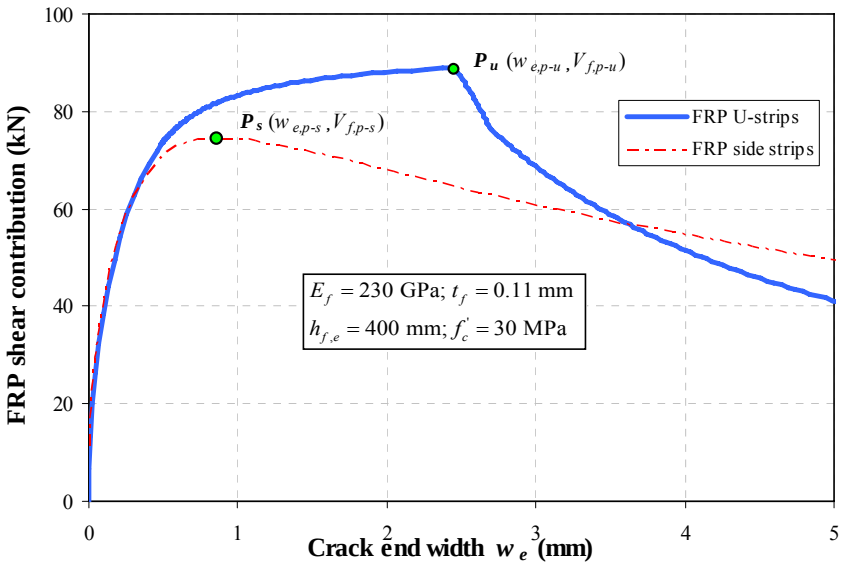

Fig. 3. Example FRP shear contribution versus crack end width

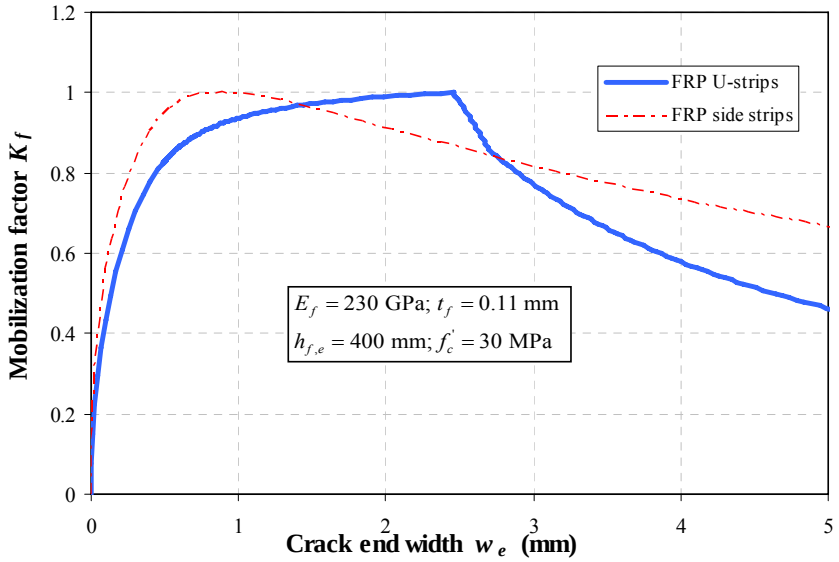

Fig. 4. Development of FRP mobilization factor

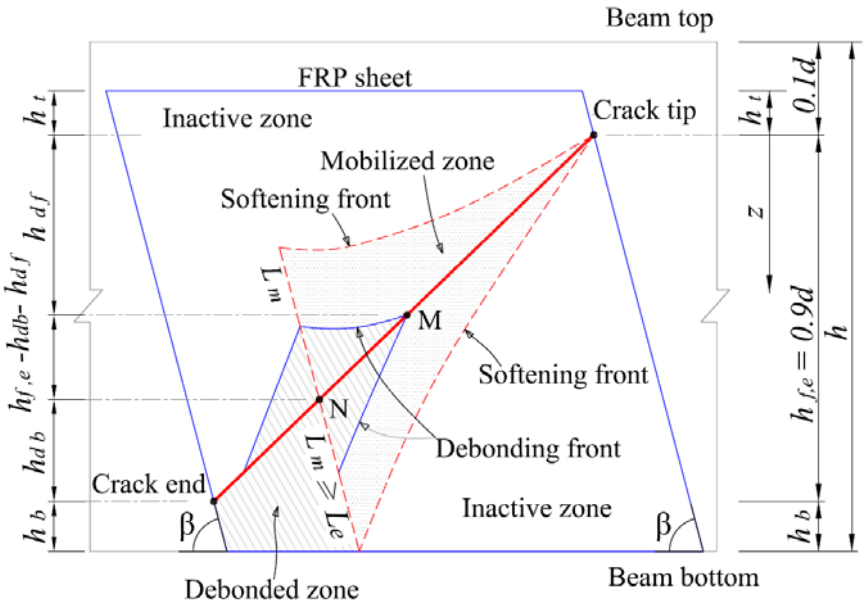

(a)

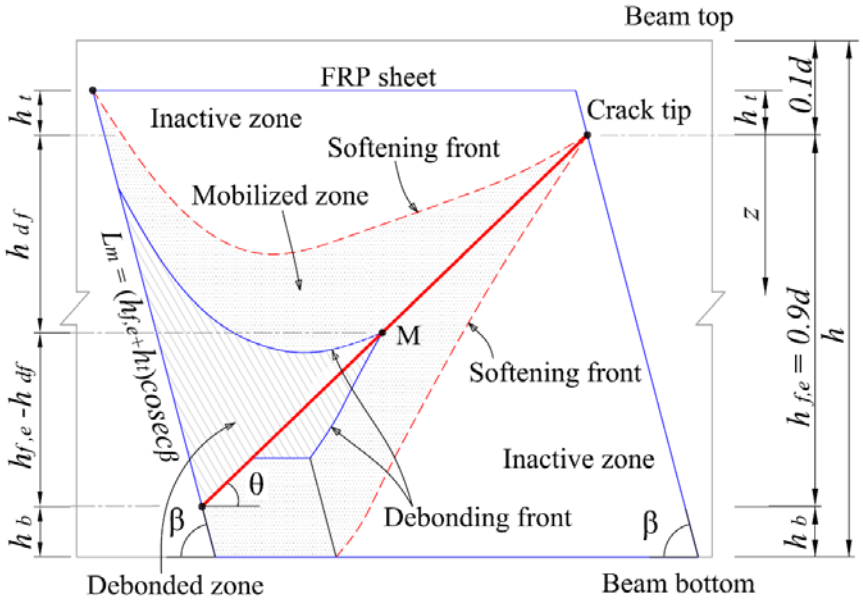

(b)

Fig. 5. Notation for the ultimate state of shear-strengthening FRP strips (Chen et al. 2011):(a) FRP side strips; (b) FRP U-strips

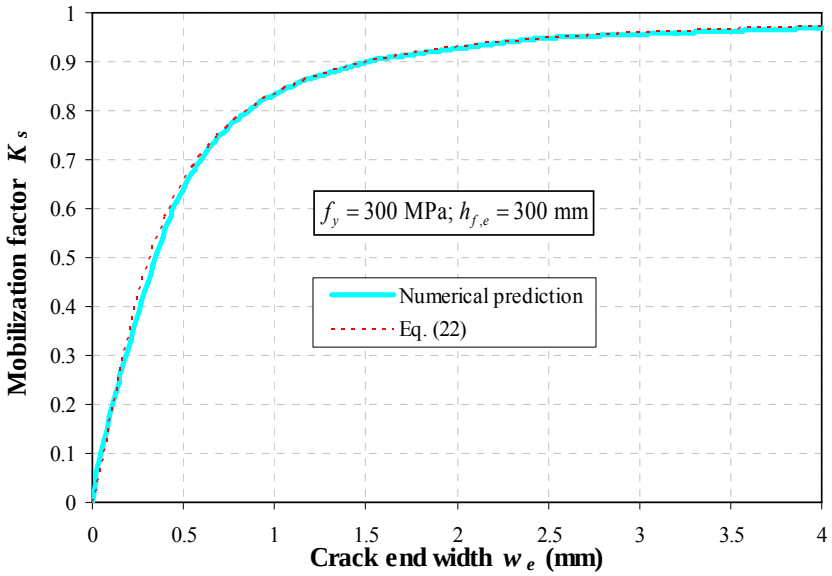

(a)

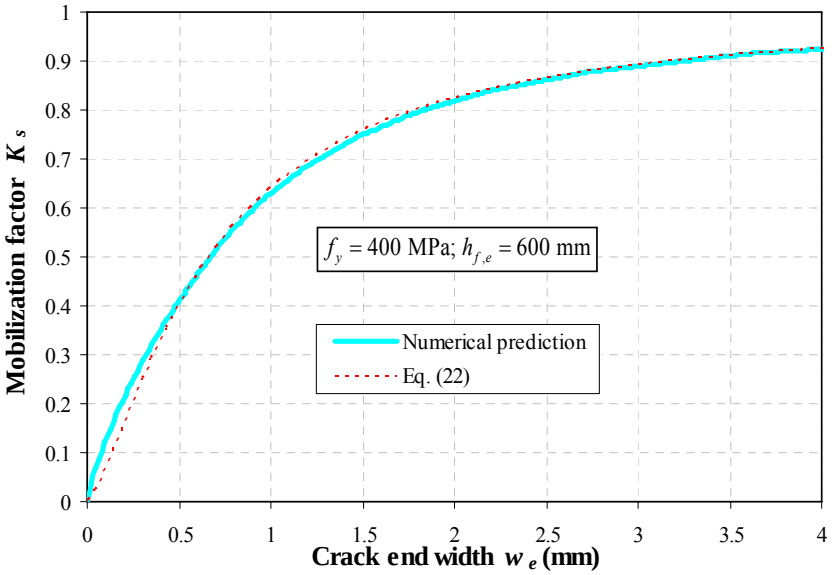

(b)

Fig. 6. Comparisons between proposed expression for K_s and numerical predictions for plain bars with $\phi_s = 8$ mm

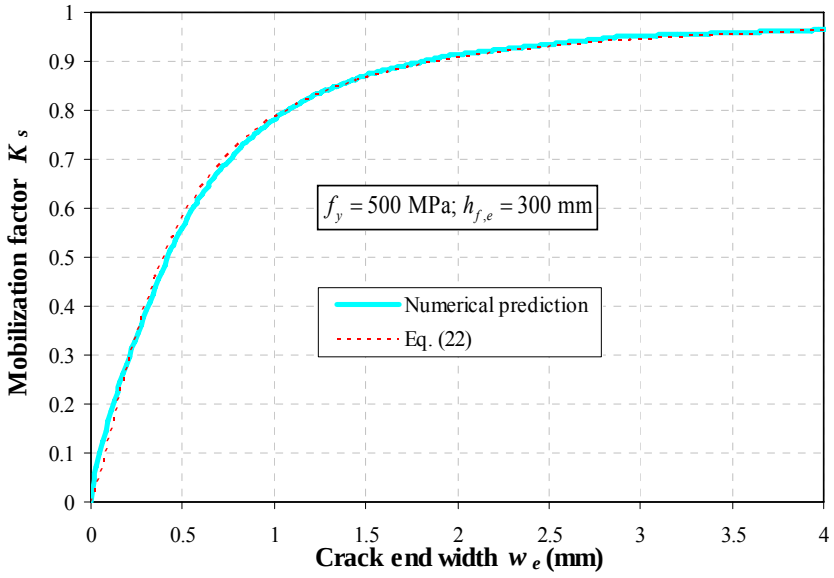

(a)

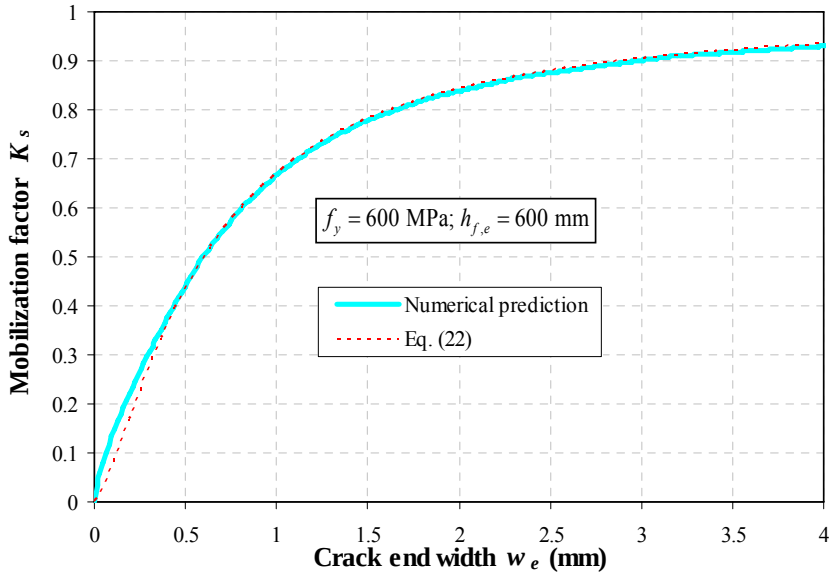

(b)

Fig. 7. Comparisons between proposed expression for K_s and numerical predictions for deformed bars with $\phi_s = 10$ mm

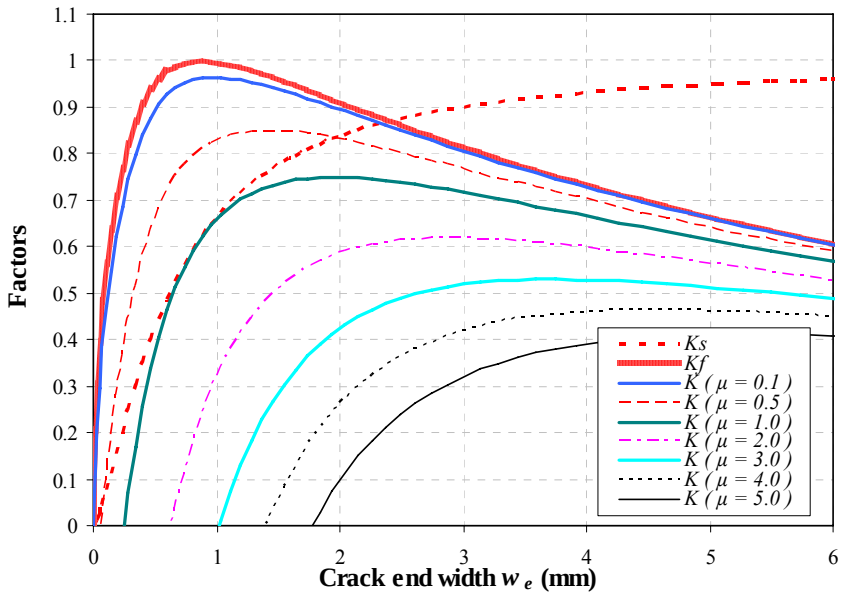

(a)

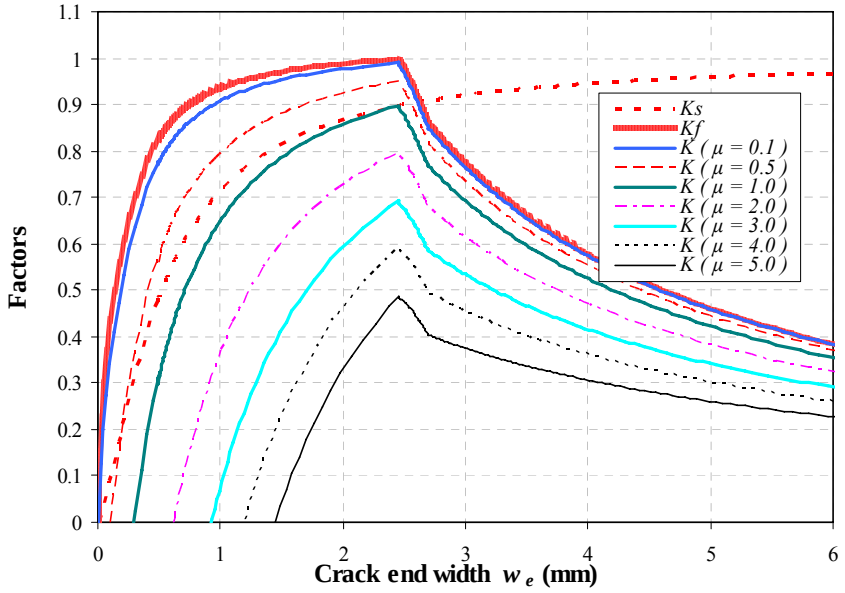

(b)

Fig. 8. Development of shear interaction factor K with crack end width w_e ($E_f = 230$ GPa, $t_f = 0.11$ mm, $h_{f,e} = 400$ mm, $f_c^{'} = 30$ MPa ; plain bars with $\phi_s = 8$ mm, $f_y = 300$ MPa): (a) FRP side strips; (b) FRP U-strips

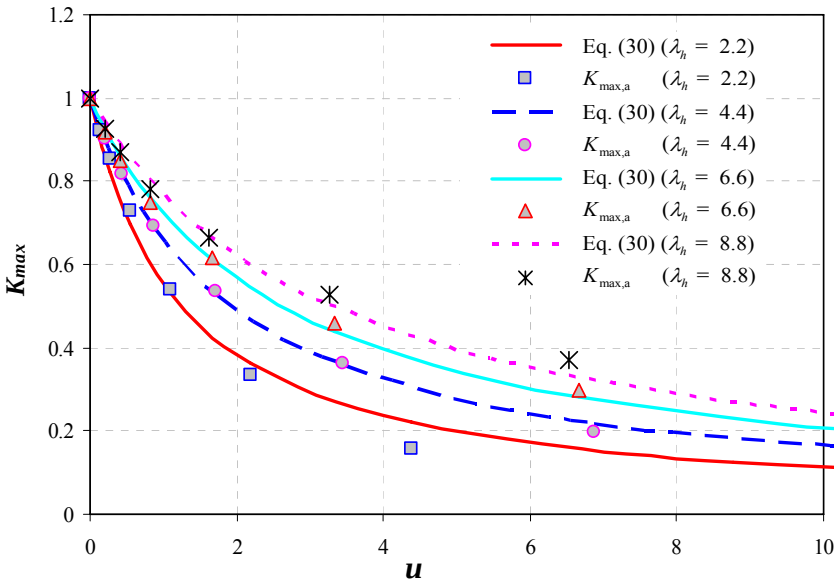

(a)

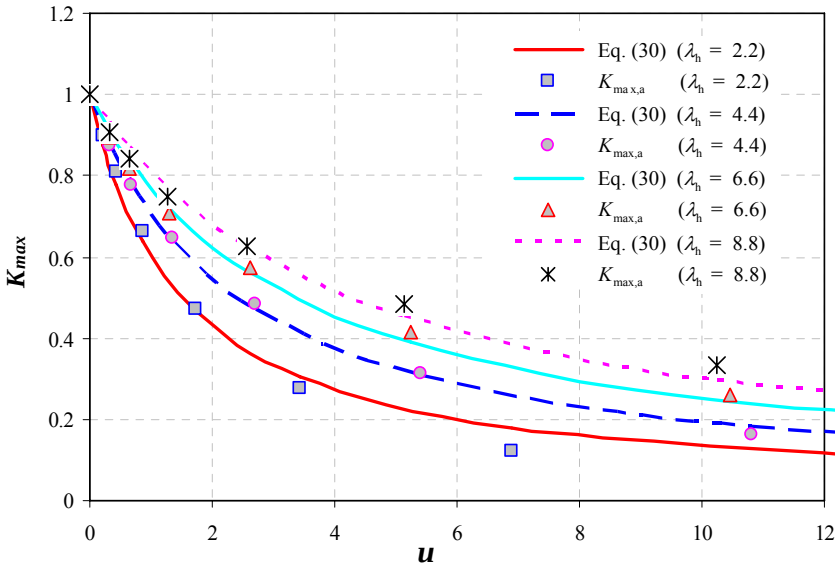

(b)

Fig. 9. Comparisons of maximum shear interaction factor between predictions of Eq. (30) and results from accurate analysis ($K_{\max,a}$) for different $\lambda_h = h_{f,e}/L_e$: (a) plain bars ($\phi_s = 8$ mm, $f_y = 350$ MPa); (b) deformed bars ($\phi_s = 8$ mm, $f_y = 550$ MPa).

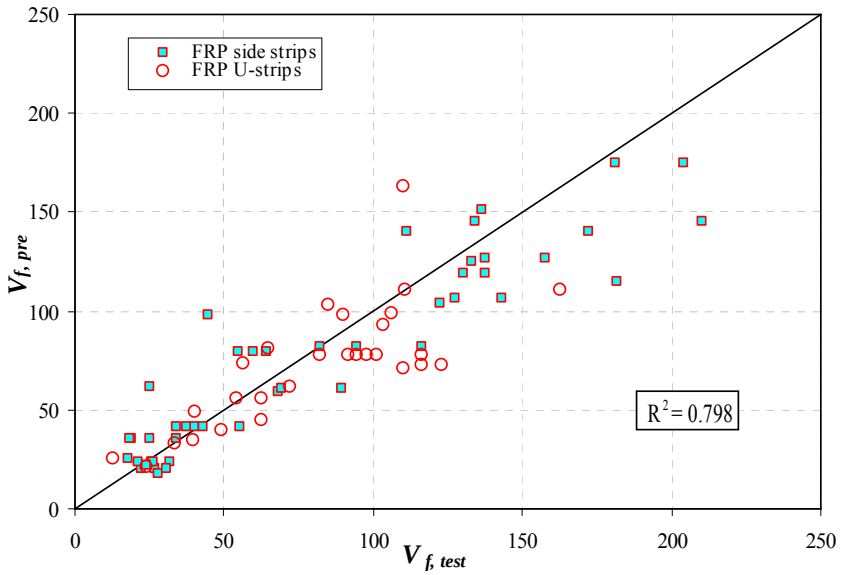
FRP side strips
FRP U-strips
$R^2 = 0.798$
$V_{f,pre}$
$V_{f,test}$
0
50
100
150
200
250

(a)

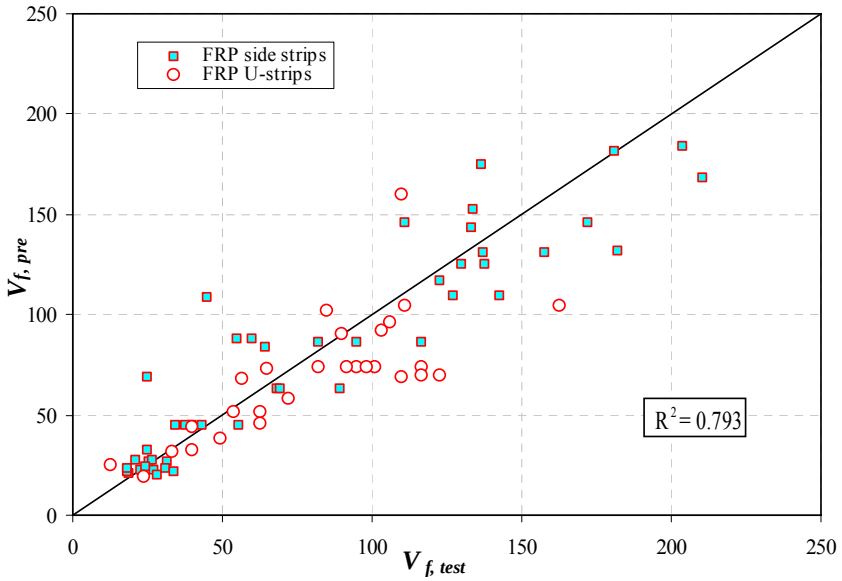
FRP side strips
FRP U-strips
$R^2 = 0.793$
$V_{f,pre}$
$V_{f,test}$
0
50
100
150
200
250

(b)

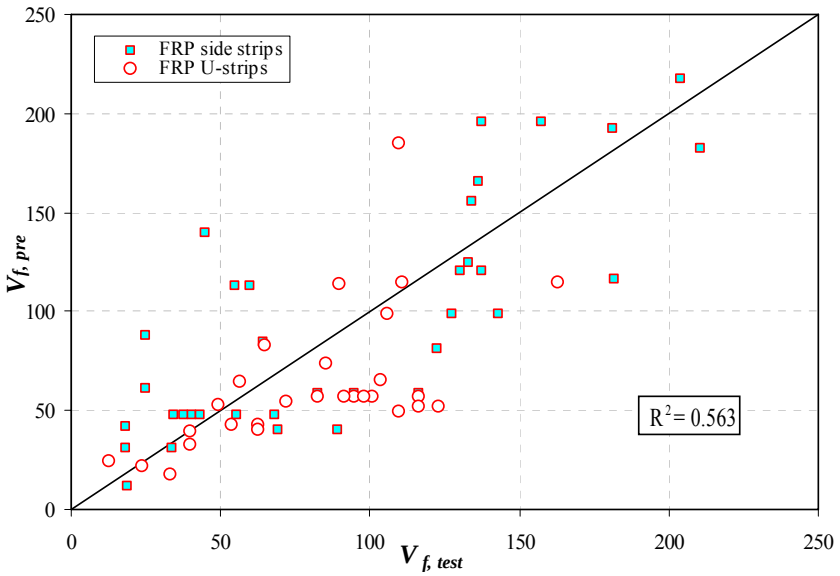

(c)

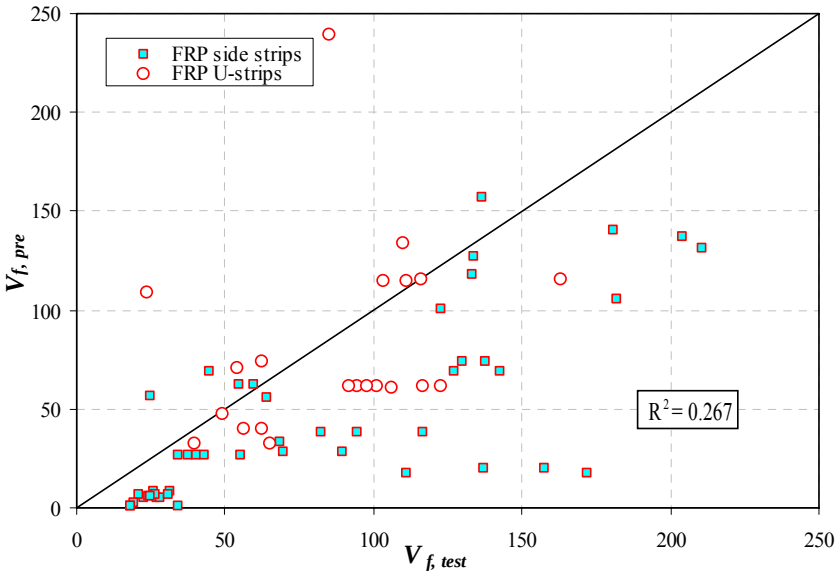

(d)

Fig. 10. Predicted versus experimental FRP shear contributions (shear interaction effect ignored) for specimens with experimental crack angles: (a) proposed model; (b) HB 305 (2008); (c) ACI 440.2R (2008); (e) CNR-DT200 (2004)

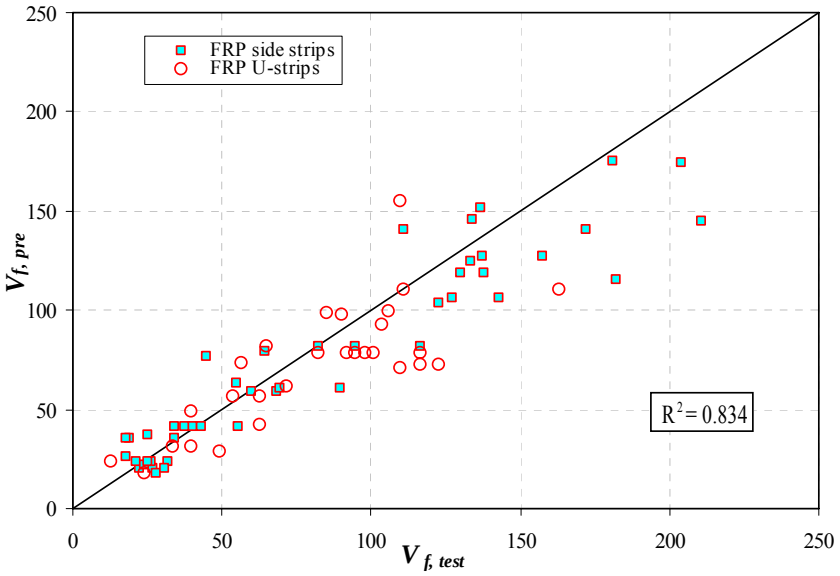
FRP side strips
FRP U-strips
$R^2 = 0.834$
$V_{f,pre}$
$V_{f,test}$
0
50
100
150
200
250

(a)

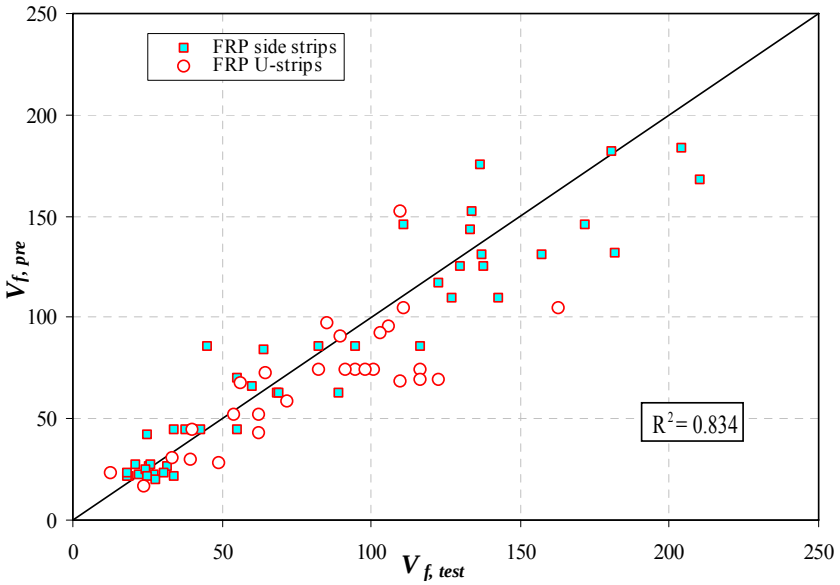
FRP side strips
FRP U-strips
$R^2 = 0.834$
$V_{f,pre}$
$V_{f,test}$
0
50
100
150
200
250

(b)

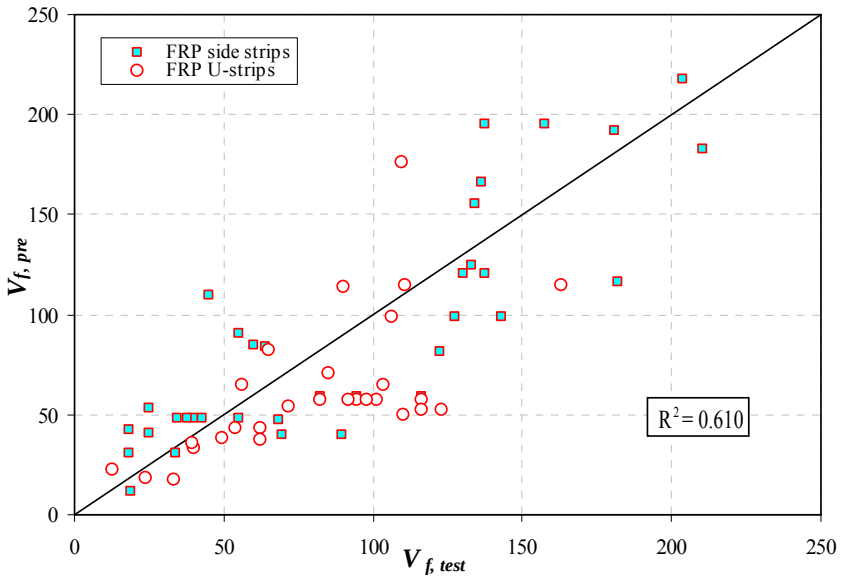

(c)

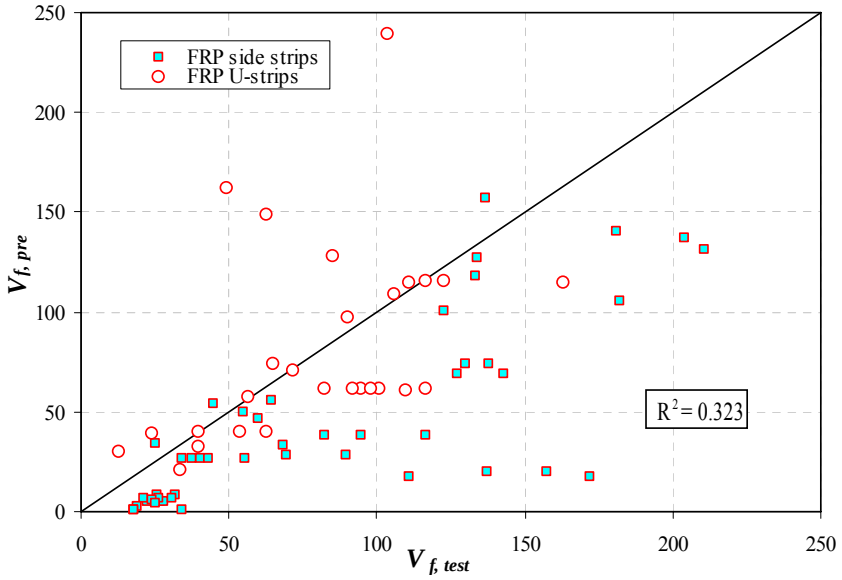

(d)

Fig. 11. Predicted versus experimental FRP shear contributions (shear interaction effect included) for specimens with experimental crack angles: (a) proposed model; (b) HB 305 (2008); (c) ACI 440.2R (2008); (e) CNR-DT200 (2004)

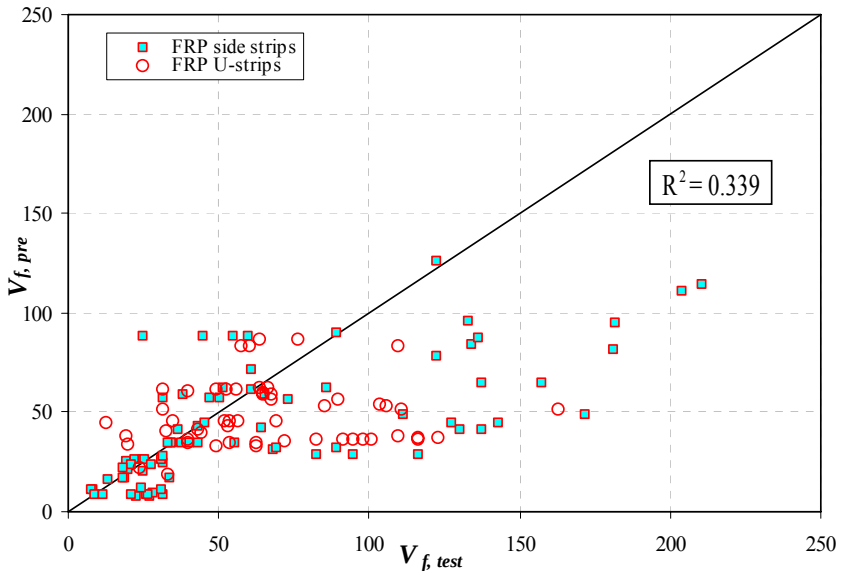
FRP side strips
FRP U-strips
R² = 0.339
Vf, pre
Vf, test
0
50
100
150
200
250

(a)

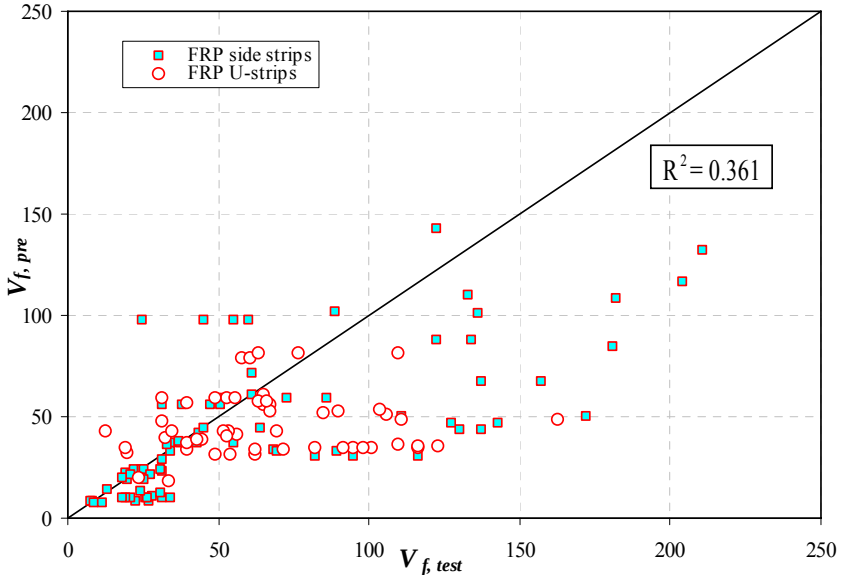
FRP side strips
FRP U-strips
R² = 0.361
Vf, pre
Vf, test
0
50
100
150
200
250

(b)

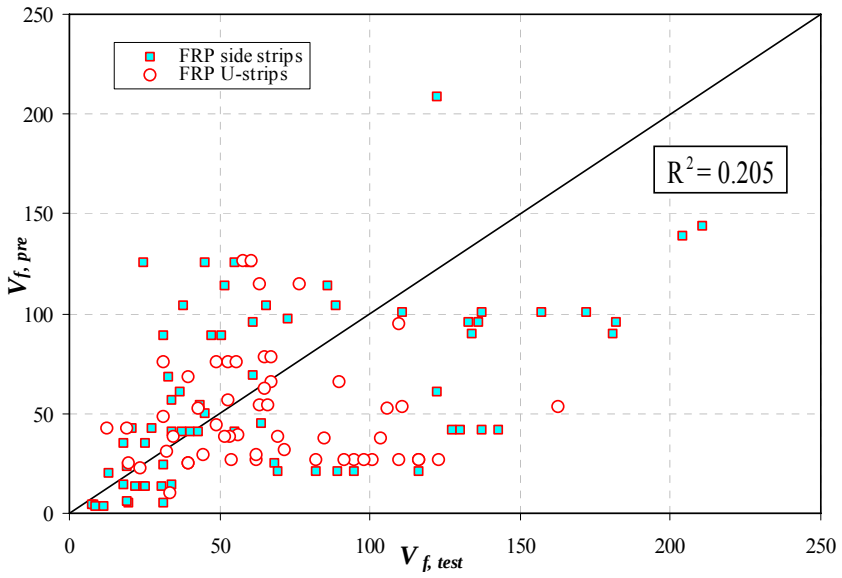

(c)

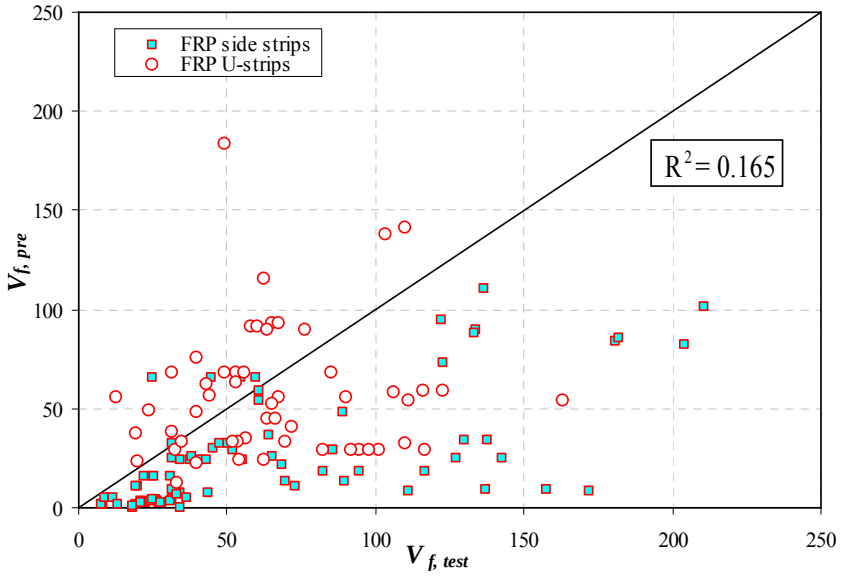

(d)

Fig. 12. Predicted versus experimental FRP shear contributions (shear interaction effect ignored) for a 45° shear crack angle: (a) proposed model; (b) HB 305 (2008); (c) ACI 440.2R (2008); (d) CNR-DT200 (2004)

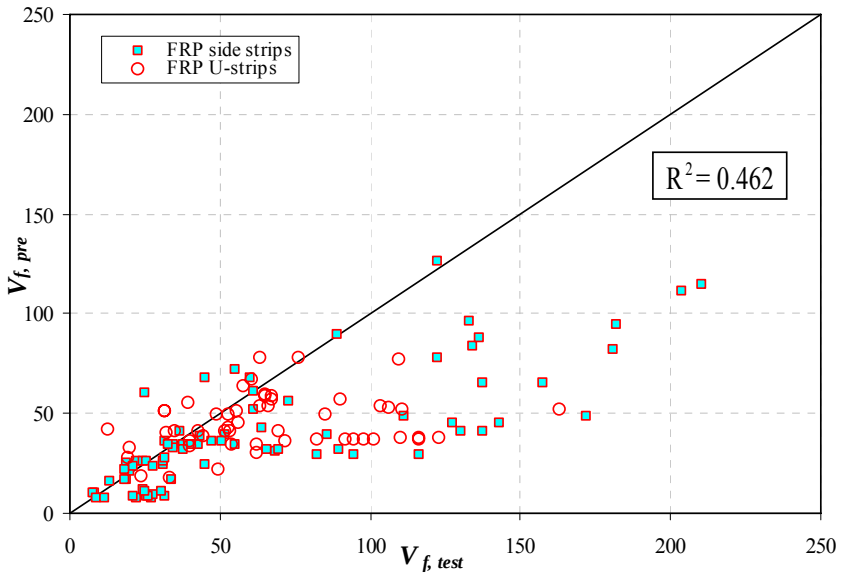
FRP side strips
FRP U-strips
R² = 0.462
Vf, pre
Vf, test
0
50
100
150
200
250

(a)

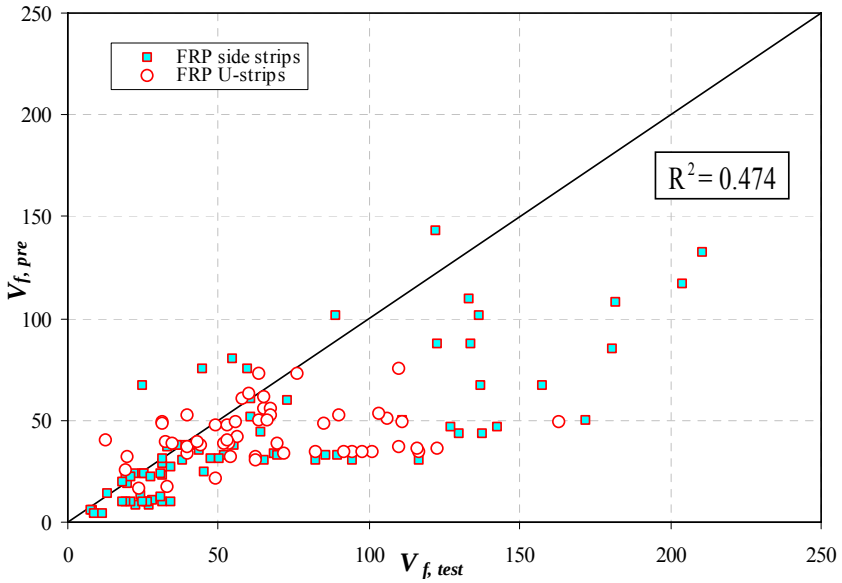
FRP side strips
FRP U-strips
R² = 0.474
Vf, pre
Vf, test
0
50
100
150
200
250

(b)

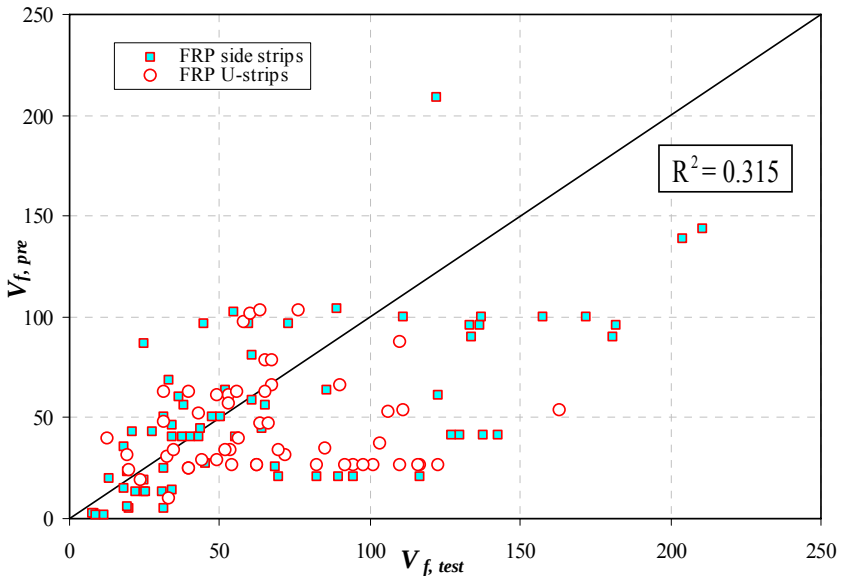

(c)

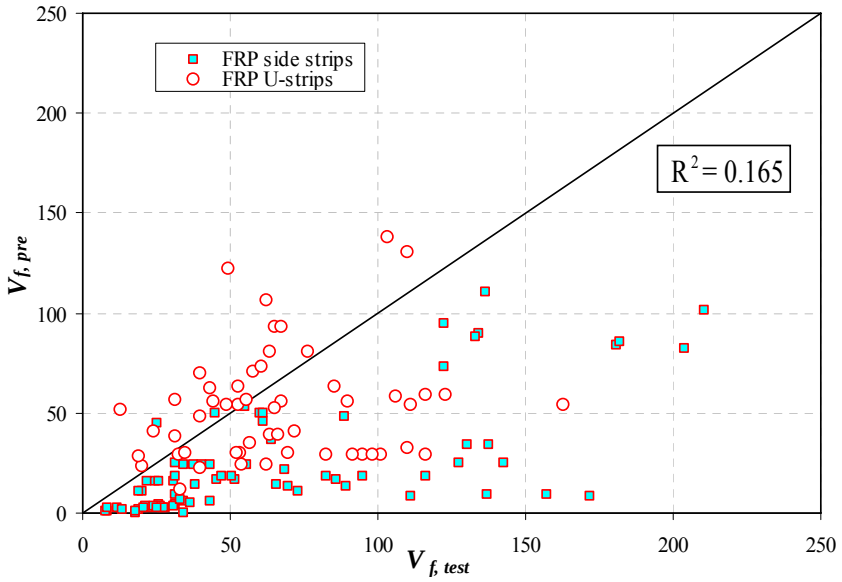

(d)

Fig. 13. Predicted versus experimental FRP shear contributions (shear interaction effect included) for a 45° shear crack angle: (a) proposed model; (b) HB 305 (2008); (c) ACI 440.2R (2008); (d) CNR-DT200 (2004)